91602
new 82-10

ontario hydro
research division

EXECUTIVE SUMMARY

ASSESSMENT OF ZIRCONIUM OXIDE ON PRESSURE TUBES; TECHNIQUE DEVELOPMENT

A.V. Manolescu
Corrosion & Tritium Technology Section
Metallurgical Research Dept

In the past, corrosion deuteriding of pressure tubes in CANDU reactors has been associated with costly and unscheduled outages.

Zr-2.5 wt% Nb (Zr-2.5 Nb) is now the only pressure tube material used in large, commercial CANDU reactors. Only limited corrosion and hydriding data exists for this alloy, and efforts are being concentrated on the development of a fuel channel corrosion and hydriding behaviour model for long-term in-reactor performance predictions under both boiling and non-boiling conditions.

To achieve these objectives, accelerated in-reactor and out-reactor tests are being carried out through a number of coordinated AECL-OHRD research programs. These tests rely on the availability of pre-oxidized Zr-2.5 Nb samples with thick oxides that have similar characteristics to those observed in-reactor after many years of operation. A fast and reliable method of sample pre-oxidation was urgently required; this program was initiated to meet this requirement.

This report is intended to update the work performed and to summarize the major achievements. Based on the work results a suitable method for preparation of the pre-oxidized coupons is recommended and an outline of future work is described.

The approach chosen was to perform morphological analysis of oxides formed on reactor pressure tubes, to determine their structural characteristics and develop a fast laboratory method to simulate these. Out of several possibilities, a method based on corrosion enhancement by increasing LiOH concentration in the

job	file	date	report no.
82-124-451	827.22	January 23, 1987	86-265-K

test solution and also raising the test temperature was selected for investigation. Since LiOH is used in the pressure tube coolant circuit for pH control, this test solution would be expected to provide a reasonable accelerated simulation environment.

From the results of this study, two test conditions were identified for the pre-oxidation of pressure tube samples. These are:

1. Tests that simulate the structural characteristics of oxide currently observed in-reactors.

   These tests were carried out in 0.5 g/L LiOH solution at 340°C. The linear rate of oxide formation was 0.1 μm/day and 0.12 μm/day for Zr-2.5 Nb β-quenched and Zr-2.5 Nb non-β-quenched material, respectively.

2. Tests that produce porous oxides which may be more similar to pressure tube end-of-life conditions.

   These tests were performed in 2.5 g/L LiOH solution at 340°C. The linear rate of oxide formation was 3.3 μm/day for Zr-2.5 Nb β-quenched material. Under these conditions a 20 μm thick scale was produced within a six-day exposure time.

Further work to improve the capability to evaluate the structural and compositional characteristics of the oxide scales formed on pressure tubes is in progress. It is believed that the results of this work will produce information that will contribute to the understanding of radiation effects on corrosion and hydriding of pressure tubes and the influence of scale spallation on fuel channel operating performance under both boiling and non-boiling conditions.

91602
new 82-10

ontario hydro
research division

To: Mr. H. Isaac
Manager, Nuclear Materials Management
Design & Development - Generation

Attn: Mr. J.S. Li
Heavy Water & Chemical Systems Engineer

ASSESSMENT OF ZIRCONIUM OXIDE ON PRESSURE TUBES; TECHNIQUE DEVELOPMENT

A.V. Manolescu

Well controlled pre-oxidized samples are required for in- and out-reactor accelerated tests designed to predict the long-term corrosion behaviour and hydriding/deuteriding* of pressure tubes. To achieve this objective, the morphology of oxide scales formed on the internal surface of pressure tubes removed from Pickering NGS "A" was analyzed and compared with that of out-reactor oxides produced under different experimental conditions in the laboratory. Based on these results two pre-oxidation procedures have been proposed to grow thick scales on corrosion samples, simulating the characteristics of in-reactor scales. Depending on requirements samples can be prepared in short-term exposures to 2.5 g/L LiOH solution or in longer-term exposures to 0.5 g/L LiOH solution at 340°C.

1.0 INTRODUCTION

Corrosion deuteriding of pressure tubes (P/Ts) in CANDU reactors has already been associated with unscheduled outages and a need for extensive surveillance and repairs.

* The terms hydriding/deuteriding will be sometimes used interchanagebly in this report. In strict terms hydriding occurs when light water out-reactor tests are involved, while deuteriding is associated with exposure to reactor heavy water.

job	file	date	report no.
82-124-451	827.22	January 23, 1987	86-265-K

The process of P/T corrosion depends principally on the type of material, operating time, temperature, water chemistry, oxide thickness and morphology dissolved oxygen in coolant and fast neutron flux.

Experience with Zircaloy-2 (Zr-2) P/Ts indicates that the rate of corrosion appears to accelerate when oxides reach a critical thickness of 15 to 20 μm. It is believed that at this critical thickness, the oxide isolates the metal/oxide interface from the bulk of the primary heat transport coolant. As a consequence, radiolytic processes in the oxide control the corrosion rate. The radiolytic processes usually enhance the corrosion rate. Under these conditions the oxide which forms is porous, and provides only partial protection against further corrosion and hydriding.

The limited information, available for Zr-2.5 wt% Nb (Zr-2.5 Nb) material, principally from analyses of selected P/Ts removed from CANDU reactors with an operating life of up to 12 years, and short-term corrosion tests in lithiated water, indicates that this material behaves differently than Zr-2.

Since the Zr-2.5 Nb is now the only P/T material used in large commerical CANDU reactors, an attempt is being made to develop reliable corrosion and hydriding data for this alloy, through coordinated OHRD-AECL, in-reactor and out-reactor, corrosion research programs/1/.

Experimental programs are underway to study the effects of radiation on corrosion and hydriding, in order to predict the in-reactor P/T performance. Carrier fuel bundles will be used to expose corrosion samples to both, boiling and non-boiling coolant/1/. In accelerated tests designed to obtain information on the rate of corrosion in the post-transition regime and establish the magnitude of the critical oxide thickness at which neutron radiation may enhance the corrosion, pre-oxidized samples are required.

Therefore, a reliable and fast method is required to prepare reproducible pre-oxidized samples with oxide scales that have similar structural and compositional characteristics as those which form in-reactor.To develop a suitable method, a program funded by Design and Development Division (NMMD) was initiated in 1985, with the objective of carrying out morphological analysis of oxide scales which form on internal surfaces of P/Ts removed from operating reactors (in-reactor), and on scales prepared in the laboratory (out-reactor), using several experimental methods.

This report is intended to update the work performed and to summarize the major results achieved. A suitable method for preparation of the pre-oxidized coupons is recommended and an outline of future work is presented.

2.0. EXPERIMENTAL INVESTIGATION

To achieve the objectives of this investigation the following approach was chosen:

1. Select and prepare samples from Zr-2.5 Nb P/Ts removed from PNGS A Units 3 and 4 for analysis. Samples from Unit 1 (Zircaloy-2) were also included for comparison.

2. Pre-oxidize P/T materials in steam (CRNL) and lithiated aqueous solutions (OHRD) to produce 10-20 μm thick, post-transition oxide in the laboratory.

3. Perform morphological and structural analysis of both in- and out-reactor formed oxides.

4. Compare the results of these analyses and recommend the most suitable method of test sample pre-oxidation.

To analyze the morphology of ZrO_2 scale that forms in-reactor on Zr-2.5 Nb P/Ts in contact with primary heat transport coolant, small samples prepared from P3-J09 and P4-N16 P/Ts were examined by optical microscopy (OM) and scanning electron microscopy (SEM) techniques. For comparison, several samples from P1-K18, Zircaloy-2 (Zr-2) P/T, were examined by OM.

To prepare oxide scales which simulate in-reactor formed scales, pressure tube material samples (cold worked Zr-2.5 Nb in β- and non-β-quenched condition) were exposed to lithiated water containing various amounts of LiOH at elevated temperatures. This is one of several methods which are being jointly investigated for the same purpose at AECL-CRNL and OHRD. The pre-oxidized samples were then examined using OM and SEM techniques.

The adherence, spalling propensity, thickness, porosity, grain size and shape of the oxide scale of in- and out-reactor samples were compared in order to establish the experimental conditions to grow oxides simulating the in-reactor scales.

2.1 Sample Description and Method of Preparation

2.1.1 In-Reactor Samples

Table I summarizes the material, the operating history and the internal surface finish of the pressure tubes that were selected

for examination. Three areas were examined on each tube: near the inlet, close to the middle and near the outlet. Table II gives the locations of the examined samples and the techniques used for their study. Selection of sample location was based on sample availability/2/.

2.1.2 Out-Reactor Samples

The samples used in out-reactor pre-oxidation tests were machined from new Zr-2.5 Nb tubes. These tubes were in the same metallurgical condition as those used in CANDU reactors, cold drawn 20 to 30%. The rectangular samples (40 x 20 x 2 mm) were cut from the tubes such that the 40 mm edges were parallel with the main axis and the 2 mm edges were parallel with the radial direction of the pressure tubes.

After machining to the required dimensions, the specimen edges were rounded off to avoid scale spalling during subsequent pre-oxidation. Following that, the specimens were pickled in aqueous solutions containing HF, H_2SO_4, HNO_3 and autoclaved for 24 hours at 400° C in steam/3/. For comparison purposes, Zr-2 samples were used in all pre-oxidation tests. The autoclaved specimens were uniformly covered with a black, adherent oxide of maximum one micrometer in thickness.

The out-reactor ZrO_2 scales of different thickness were formed by exposing the autoclaved samples to LiOH solutions in static autoclaves at 300-360°C for varying time periods. Table III summarizes the experimental parameters that were selected to grow scales of different thicknesses. To the end of May 1986, only some of the parameters were investigated. Those examined are discussed in Section 3 (Results and Discussion).

The LiOH solutions were prepared by adding weighted amounts of the base (LiOH 99% pure, BDH Cat No B29073-34) to de-ionized, degassed water. Room temperature pH values were measured prior to, and immediately following each test cycle using a Fisher Accumet No 325 pH Meter equipped with a Fisher Combination Electrode No 31-639-90. The values of pH before and after the tests were found to vary within 0.5 of a pH unit. No attempt was made to control, or measure pH at the test temperature. Table IV gives the relationship between the concentration of LiOH in solution and pH at RT.

Figure 1 shows a schematic of autoclave and sample arrangements. Before each test, the weighed autoclaved samples were suspended from the liner on Zr-2 wires, and the whole vessel was purged with 5.29 vol% H_2-He gas mixture for at least 3 hours. The onset of the test was considered to be the instant when the sealed autoclave reached the operating temperature.

In addition to specimens prepared at OHRD in LiOH solutions the morphology of a thick oxide scale formed on Zr-2.5 Nb non-β-quenched sample in steam (CRNL) was also examined.

2.2 Techniques for Sample Analysis

2.2.1 In-Reactor Oxide Samples

Both OM and SEM techniques were used for examination of the oxide scale on the internal surface of the P/T samples. Cross sections for metallographic examination were prepared by mounting the P/T samples in epoxy (P4-N16 and P3-J09) or in silica containing epoxy (P1-K18)/2/. Standard grinding and polishing techniques were used to prepare the mounted cross sections for examination under the optical microscope. Minimum pressure was applied on the specimens during sample preparation to avoid breaking and/or cracking the oxide scales. Then, micrographs were taken from the most representative area under the optical microscope. Corrosion advancement was estimated from the thicknesses of the oxide scales that were measured with an optical microscope equipped with reticule. The metallographically prepared cross sections were then etched in solutions containing lactic, nitric, and hydrofluoric acids, and optically examined to determine the hydride distribution under the metal/oxide interface.

For the first time, a special technique for SEM examination of irradiated P/T samples was used by AECL-WNRE in collaboration with OHRD. Samples for SEM examination were obtained by cutting thin strips from the pressure tubes. Three or four saw cuts (3.5 mm deep) were then made on the outside surface and the samples bent in the outward direction to fracture the oxide on the internal surface. These samples were then gold-coated by vapour deposition and the fracture surface examined under the SEM. Figure 2 illustrates schematically the SEM sample configuration. Figure 3 shows the appearance of the fractured oxide scale on the internal P/T surface.

2.2.2 Out-reactor Samples

The morphology of out-reactor samples was also analyzed by OM and SEM. The same metallographic techniques, as those described for in-reactor samples, were used for sample preparation and examination. In addition to microscopic examination, the internal oxide surface area of selected oxidized samples was measured. The suitability of the gas absorption technique for ZrO_2 internal surface area measurements was evaluated. This work was performed at Ontario Research Foundation with a Micromeritics Orr Model 2100 SA Analyzer. The technique consisted of

admission of Krypton gas to a sample of known weight and thickness, which has been previously dried, weighed and freed of absorbed gases and vapours. The surface area was calculated from the volume of the gas absorbed by each sample.

3.0 RESULTS AND DISCUSSION

3.1 In-Reactor Scales on Zr-2.5 Nb Pressure Tubes

3.1.1 Scale Surface Appearance

The optical micrographs in Figures 4 and 5 show the inside surfaces of the examined P/Ts. No obvious differences in the internal surface appearance are discernible between the two P/Ts or different locations on the same P/T. The surfaces appear rough at 50X. This roughness is apparently a result of the sandblasting operation which was performed during the manufacturing process of the P/Ts before autoclaving/2/.

3.1.2 Scale Integrity and Morphology

Typical cross sections of the oxide scales at examined locations are illustrated in Figures 6 and 7 for P3-J09 and P4-N16 P/Ts, respectively. The scales consist of a one-layer homogeneous oxide and show excellent adherence to the internal surface of the P/Ts. No gaps or cracks were observed at the metal/oxide interface to indicate physical separation on examined samples. The adherence of the oxide to the metal is the reason why zirconium alloys exhibit a remarkable corrosion resistance and excellent performance in nuclear and other industrial applications. Although this property at the metal/oxide interface is never lost, the integrity of the bulk oxide scale may break down under certain conditions leading to enhanced metal wastage.

However, on all examined samples/2/ the outer surface of the oxide, at the oxide/coolant interface, was irregular and rough due to a non-uniform spallation (detachment or sloughing of small portions of the scale). The arrows in Figures 6 and 7 indicate some areas where severe oxide spallation took place. The most severe damage associated with scale spallation was observed at the outlet end of P4-N16 tube (Figure 7E). Spalling of oxide scales formed on internal surface of P/Ts removed from CANDU reactors was previously reported/4,5/.

From the present examination, it appears that the scale spallation took place at locations where extensive cracking of the oxide was observed. Two types of cracks were identified in the scale: parallel and perpendicular to the metal/oxide interface. Most of the perpendicular cracks penetrate only about

half way through the oxide scale; a few penetrate the scale deeper but do not reach the metal/oxide interface.

In general, cracking and spalling of oxide scales, which form on metals and alloys at elevated temperatures, are the result of stresses that accumulate in them during growth and/or are imposed on them by thermal cycling and system operating pressures. Growth generated stresses are due to the fact that the oxide scale occupies a larger volume than the metal from which it has been formed.

In the oxide which forms on zirconium and zirconium alloys, the main source of stress is probably the high volume of ZrO_2 when compared with the volume of the metal it originates from. This places the oxide in compression and, simultaneously, imposes tensile stresses on the underlying metal. To relax these stresses, the oxide cracks laterally (parallel with metal/oxide interface)/6/ and/or recrystallizes/7,8/. The oxide recrystallization is associated with development of a fine network of pores in the oxide scale/9/.

The perpendicular cracks could be associated with stresses which arise due to differences in thermal expansion coefficients of the metal and oxide. Work by Cox/9/ suggests that the cracks observed in metallographic samples may be at least partly produced during the sample preparation. As a result there is no easy way to ascertain the actual origin of observed cracks. This uncertainty can only be reduced by the further development of oxide examination techniques and skills. New techniques must be developed and applied.

3.1.3 Scale Grain Structure

Although the oxide scales appeared homogeneous under the optical microscope, the real grain structures were revealed by examining the fracture surfaces of the scale under the SEM. Figures 8-11 illustrate typical observations at different magnifications.

The low magnification SEM micrographs in Figures 8 and 9 show that the outer surface of the scale was rough and irregular; the arrows in Figures 8A, 8C, 9A, 9B and 9C indicate the presence of large voids on the outer surface of the scale.

The SEM micrographs shown in Figures 10 and 11 illustrate, at high magnification, the structure of the oxides. The oxides consist of grain clusters and/or individual fine grains. These features are pencil-enhanced on the micrographs. This type of structure provides interconnected porosity, mainly at triple points, where the individual grains meet.

Samples from the outlet end of P4-N16 (Figures 11D and 11F) exhibit some regions with a more developed crystalline structure consisting of randomly oriented columnar grains. For easy location of these in the micrographs the contours of these grains were pencil-enhanced. Although a special effort was made to establish the oxide structure at the metal/oxide interface, the examinations were not successful. This may be indicative of a partially amorphous nature of the oxide at this location or the lack of a suitable examination technique.

The size of the observed grains ranges from less than 0.1 to 0.3 μm. In most of the examined samples, some larger grains at the outer surface than throughout the scale were identified.

It is difficult to explain this above finding, since it was expected that at the outermost surface, the location of the oldest oxide, the scale would consist of smaller grains resulting from an oxide nucleation process which occurs during the initial stages of the corrosion process. The oxide in the middle of the scale and at the metal/oxide interface is subjected to the highest growing stresses and is expected to consist of grains of different sizes resulting from recrystallization and grain growth processes. Thus, it is possible that the outer oxide surface (oxide/coolant interface) found in this work consisting of large grains, is in fact, not the original surface. The oxide which formed initially on the P/T surface may have spalled during operation and/or sample preparation. The oxide structure observed may be typical of what would have been expected in the bulk of the scale.

3.1.4 Extent of Corrosion

Because it is not possible to determine exactly the degree of spallation for the examined scales, the extent of corrosion cannot be established from the scale thickness with any confidence. Therefore, only the maximum thicknesses of the scales that were found adhering to these P/T samples are reported. These are given in Tables V and VI.

3.1.5 Hydride Distribution

Etching of the metallographically prepared cross sections revealed the hydride distribution in the metal of the P/T samples. Figures 12 and 13 show typical hydride structures under the oxide scale on the internal P/T surface at examined locations; a low number of small hydrides was observed.

3.2 In-Reactor Scale on Zircaloy-2 P/T

Figure 14 shows the surfaces of P1-K18 P/T samples that were used in this examination. No obvious differences in the

internal surface appearance were identified at the examined locations: close to the inlet, in the mid-section and close to the outlet of the P/T.

The P/Ts used in Pickering NGS Units 1 and 2 were pickled as part of their manufacturing process. This led to an initially smooth inside surface, unlike the sandblasted Zr-2.5 Nb tubes/2/.

The micrographs in Figure 15 show the typical cross sections of the oxide scale at the three examined locations.

The internal surface of the tube was covered with a thick oxide scale that exhibited excellent adherence at the tube internal (metal/oxide interface) surface. At a few locations, the outer surface (scale/coolant interface) was irregular indicating some oxide spallation; some of these locations are marked with arrows in Figure 15. The scales on Zr-2 P/T appear to suffer somewhat less from spallation since the oxide/environment surface has a more uniform, regular appearance than that of Zr-2.5 Nb P/Ts. The scales exhibit cracking similar to that observed in Zr-2.5 Nb P/T samples. The micrographs in Figure 15 illustrate some parallel and perpendicular cracks.

The maximum oxide thicknesses identified at the three examined locations are given in Table VII. The thickness of the scale increases along the P/T, with the thickest oxide scale identified near the outlet end. The oxide scales found on Zr-2 P/T surface are significantly thicker than those observed on Zr-2.5 Nb samples.

The hydrides in the P/T metal near the inlet end of P1-K18 were large (Figure 16), randomly oriented and evenly distributed. Near the outlet end, a higher density of larger hydrides was observed, with more hydrides aligned in the circumferential direction (Figure 16).

3.3 Out-Reactor Scales on Zr-2.5 Nb Laboratory Samples

3.3.1 Scale Surface Appearance

The results of visual examination of the samples after corrosion testing are summarized in Table VIII. Except for the tests in 0.5 g/L solution at 340 and 360°C, only white oxide scales were observed. In the 0.5 g/L solution, hard compact, grey colored (mixture of dark grey and white) oxide developed. Figure 17 illustrates the appearance of the oxide scale which formed in solutions containing 0.5, 2.5 and 10 g/L of LiOH. Since only the scales formed on what was originally the internal surface of the P/Ts are of interest the external surfaces were not examined

in detail. However, the scales on the external surfaces appeared more tenacious (Figure 18) than on the internal surface.

The visual examination also revealed that the β-quenching step in the P/T fabrication process was associated with a reduced tendency of the friable scales formed in concentrated solutions to spall off (Figures 17 and 18). Testing of additional β-quenched tube material is planned to confirm this observation.

3.3.2 Scale Integrity and Morphology

The results of OM examination of out-reactor samples produced under different experimental conditions are illustrated in Figures 19 to 21 and summarized in Table VIII. The test conditions are shown for each examined sample on the right side of each micrograph (Figures 19 and 20). All examined scales consisted of homogeneous one-layer oxide and showed excellent adherence to the metal. No gaps or cracks were observed at the metal/oxide interface to indicate physical separation. This structural characteristic is the same as that observed in examination of in-reactor oxides. Thus, the out-reactor scales prepared in LiOH solutions simulate the structural features of the in-reactor oxides at the metal/oxide interface.

The oxide compactness was found to depend on the LiOH concentration and exposure time. The effect of increasing LiOH concentration is illustrated in Figure 19; the scales gradually loose their compactness and became powdery. Time of exposure to test solution has a similar effect (see Figures 19C and 21A). Visual comparison of the out-reactor oxide cross sections with those of in-reactor oxide indicates that the oxide formed in 0.5 g/L LiOH solution appears to have the compactness of the in-reactor oxide. This oxide is dense and shows excellent adherence to both flat surfaces and rounded corners of the samples as illustrated in Figures 19A and 20. Based on these observations it is believed that oxides simulating in-reactor oxides can be produced successfully out-reactor in 0.5 g/L LiOH solutions.

Similar to in-reactor scales the oxides produced in LiOH solution show a tendency to spall at their outer surface, from cracks parallel with the metal/oxide interface.

The effect of the β-quenching step in the manufacturing process of the P/Ts on scale integrity is illustrated in Figure 21. The oxide grown in 2.5 g/L LiOH solution at 340°C was found more compact and less flaky on β-quenched than on non-β-quenched Zr-2.5 Nb samples.

The cross sections in Figure 21 show also that oxides that formed on what were originally external surfaces of the P/Ts are less porous than those observed on originally internal surfaces. This phenomenon was observed for both β-quenched and non-β-quenched Zr-2.5 Nb samples.

3.3.3 Scale Grain Structure

Figures 22 to 24 show the scanning electron micrographs of the fracture surface of out-reactor oxide scales formed in 0.5, 2.5 and 4.0 g/L LiOH solutions at 340°C.

The bulk of the oxide formed in 0.5 g/L LiOH solution consists of fine equiaxed grains ranging in size from less than 0.1 to 0.3 μm (Figure 22). At some locations columnar grains were also observed. These structural features were pencil enhanced in the micrographs. At the outermost surface of the oxide, the equiaxed grains seem to be smaller in size than throughout the scale. This location is indicated by arrows in Figure 22. The observed structural features of the oxide are consistent with the assumption, mentioned in Section 3.1.3, that the oxide which forms first on a zirconium alloy surface is expected to have the smallest grain size. Because of the technique limitations it was difficult to examine the oxide microstructure near the oxide/metal interface.

The scale formed in 2.5 g/L LiOH solution has the same granular structure but is less compact (Figure 23).

Figure 24 shows that the oxide formed in 4.0 g/L LiOH solutions consists of loose agglomerates of small, approximately spherical grains providing a high porosity.

Visual comparison of the grain structures of out- and in-reactor oxides indicates that the oxide formed in 0.5 g/L solution appears to have a structure resembling that of in-reactor scales.

3.3.4 Extent of Corrosion

The thickness of oxide scales formed under investigated experimental conditions was both calculated from the corrosion weight gain and measured metallographically. These results are summarized in Table VIII.

The thickness of the oxide was calculated from observed weight gain of each sample using the formula*:

$$\Delta w = 14.6 \times h$$

where Δw is the weight gain per unit area (mg/dm^2) and h is the calculated thickness of the oxide (μm).

The thickness of the oxide was measured directly on metallographically prepared samples under the optical microscope equipped with reticule.

For flaky, loose oxide scales only the calculated thickness is reported.

The results of these measurements suggest that Zr-2.5 Nb non-β-quenched material corrodes faster than β-quenched material under all investigated experimental conditions.

The values of calculated oxide thickness in all cases are lower than those measured metallographically. The difference between calculated and measured values of scale thickness increases with increasing LiOH concentration in test solution and exposure time. This suggests that the scale porosity increases with an increase in the environment corrosivity, since the formula used to calculate the oxide thickness from weight gain assumes 100% oxide density.

3.3.5 Hydride Distribution

The micrographs in Figure 25 show the size distribution and density of hydrides in samples exposed to 0.5 g/L LiOH solution. The hydrides appear to have similar characteristics as those observed in the in-reactor exposed P/T samples.

3.4 Out-Reactor Scales on Zircaloy-2 Laboratory Samples

Visual examination of the test samples revealed that after corrosion test completion, all samples were covered with an adherent, uniform, black coloured oxide scale.

The micrographs in Figure 26 show a typical cross section of the oxide formed on Zr-2 after a 26-day exposure at 340°C to 0.5 g/L LiOH solution and a 9-day exposure at 340°C to 2.5 g/L LiOH solution. The scales consist of homogeneous and compact one-layer oxide well adhered to the metal. Both these scales appear to exhibit the gross general features of the in-reactor

* Formula is based on a density of 5.7 g/cm^3 for monoclinic ZrO_2.

ZrO_2 scales. More detailed SEM examinations would be required to confirm this observation.

The scales formed in more concentrated LiOH solutions show some tendency to spall due to formation of parallel cracks. Nevertheless, the ZrO_2 scales formed on Zr-2 are significantly more compact and have a lower tendency to spall than the scales on Zr-2.5 Nb materials.

The micrographs in Figure 27 show the hydride distribution under the oxide scale formed in 0.5 g/L LiOH (Figure 27A) and 2.5 g/L LiOH (Figure 27B) solutions. A high density of large hydrides was observed under all experimental conditions.

3.5 Out-Reactor Steam-Formed Scale

A Zr-2.5 Nb non-β-quenched sample after two months exposure in steam at 490°C (CRNL) was also examined. Visual examination showed that the sample was covered with uniform adherent, dark grey coloured scale. The micrographs in Figure 28 illustrate the scale morphology and hydride distribution under the oxide scale. The scale spalled-off at the sample corners as indicated by arrows in Figure 28. Vertical cracks penetrating to the metal/oxide interface were observed. These cracks developed probably due to thermal cycling during sample preparation.

The SEM examination shows that the steam-formed scale is very compact (Figures 29 A and B), and consists of long columnar grains. At random locations some equiaxed grains are also observed. These are pencil-enhanced in Figure 29. The oxide grains are larger on the internal compared with the external surface of the P/T sample.

The results of the present investigation indicate that the steam-formed scale is more compact than the in-reactor scales and has a different grain structure. The hydride size and density is also different than those observed in P/Ts removed from reactor; a very high density of large hydrides was observed.

3.6 Scale Porosity

The porosity of ZrO_2 scale which forms on zirconium and zirconium-based alloys is related, in general, to the corrosion rate, environmental conditions (pH, temperature, O_2, etc) and metallurgy of the alloy (structure, impurity distribution and phase composition, etc).

In neutral or slightly alkaline solutions, at nuclear reactor operating conditions, the oxide porosity for a given material is

related to the corrosion advancement characterized by two regions or periods which are often referred to as pre-transition and post-transition or break-away. The duration of each period depends on the environmental conditions and alloy metallurgy. At transition, the normally protective bulk oxide becomes porous and prone to spalling. The reason for this transition is the inability of ZrO_2 to withstand growth and other stresses. These stresses induce formation of parallel cracks/6/ in the oxide or lead to its recrystallization/7-9/ which causes development of a network of very fine pores. The originally highly protective scale becomes permeable to reactant species. In general, the higher the porosity, the higher the corrosion rate.

Experience with Zr-2, indicates that in the fast neutron radiation environment additional enhancement of the corrosion rate may occur when the oxide scale reaches a critical thickness of 10-15 μm. It is postulated that at this thickness, the mixing of the bulk coolant, and the coolant in the pores is prevented and the radiolytically produced oxygen enhances the corrosion reaction/10,11/.

If the effects of porosity as described above, are a major factor in Zr-Nb corrosion, than in order to produce oxides that really simulate the in-reactor scales, the out-reactor formed oxide must also have the same porosity, and all other oxide characteristics must be as similar as possible.

Very porous scales like those formed in concentrated LiOH solutions (4 to 24 g/L of LiOH) usually have a strong "memory" effect and corrode at an accelerated rate/12/. Very compact scales (formed in steam) with a lower porosity than in-reactor scales and with a predominantly columnar grain structure would be predicted to produce incomplete information related to the value of critical thickness and radiolytical processes that take place inside the oxide pores. Thus, these scales may not be well suited for accelerated in-reactor tests.

At present, there are several techniques that have been used to characterize the porosity of ZrO_2 produced in out-reactor tests on Zr-2 alloy/13-16/.

In general, the geometric characteristics, that describe a porous structure are: surface area of pores, total pore volume and pore size distribution.

For the purpose of technique evaluation, the specific surface area of a limited number of out-reactor oxides formed under different experimental conditions (from this and other investigations/17/) was measured using the method described in Section 2.2.2. The results of these measurements are summarized

in Table IX. These results indicate that this method may be a useful tool for ZrO_2 porosity characterization. The measurements support the results of OM and SEM examinations; the scales formed in increasingly concentrated LiOH solutions are increasingly porous and Zr-2 scales are less porous than Zr-2.5 Nb scales.

Because of their high activity no attempts were made to characterize the porosity of oxide scales on P/Ts, removed from operating reactors using a gas absorption technique.

In the future, consideration should be given to the further development of this technique for use on in-reactor oxides, so that their porosity can be more accurately compared with the out-reactor oxides.

The pore volume and size distribution cannot be easily measured by OM and SEM in a quantitative manner. The TEM technique which may be more suitable was not used since it requires at this time, development for quantitative use in our laboratory. TEM technique development will enable us to obtain not only information about the porosity but also about the surface defects, structure and composition of the oxide and metal close to the metal/oxide interface.

A simple way to estimate the porosity volume is to compare the scale thickness calculated from the weight gain and the average scale thickness that was measured under the optical microscope equipped with a reticule. The data shown in Table VIII indicate that in all cases the values of oxide thickness measured metallographically, are higher than those calculated assuming theoretical density of ZrO_2. The difference between these two values is the total volume of oxide pores. The calculated apparent pore volumes of oxide scales formed in different laboratory corrosion tests are given in Table X. The findings confirm the qualitative results of the SEM examination; the scale porosity decreases with decreasing LiOH content in the test solution; the most compact scales are those obtained in steam oxidation.

4.0 SUGGESTED METHOD TO PRODUCE SIMULATED THICK OXIDES FOR IN-AND OUT-REACTOR ACCELERATED TESTS

The results to date demonstrate that oxides which simulate the structural characteristics of currently observed in-reactor oxides could be produced in the laboratory. Based on the test results reported here a fast and reliable method to accelerate the oxide growth by a moderate increase in LiOH concentration in the test solution and test temperature was identified. The following experimental conditions were established:

- test solution - 0.5 g/L LiOH in water

- temperature - 340°C.

Under these experimental conditions the corrosion rates required to produce certain oxide thickness were calculated assuming linear relationships between time and corrosion advancement. These rates were 0.1 and 0.12 μm/day for β-quenched and non-β-quenched Zr-2.5 Nb materials, respectively. A 10 μm scale simulating the most important properties of the in-reactor scales, can be produced in a three-month exposure. To attempt to shorten the exposure time further tests will be carried out under similar conditions at 360°C. In addition, thick oxide scales with similar characteristics to in-reactor oxides, but more porous, could be prepared under the following conditions:

- test solution - 2.5 g/L LiOH solution

- temperature - 340°C.

The linear corrosion rate calculated for scales formed on Zr-2.5 Nb β-quenched samples was 3.3 μm/day. Under these conditions, a 20 μm scale was produced in a 6-day test. Because of their higher than in-reactor oxide porosity these pre-oxidized samples are suitable for studies simulating P/T end-of-life conditions.

The work to assess and compare the in-and out-reactor scales continues. The out-reactor pre-oxidized samples and small in-reactor (P/T) samples are presently being re-exposed (AECL, OHRD) in static autoclaves to simulated PHTS coolant to evaluate and compare their memory effects following exposure to accelerating conditions, ie higher than expected oxide growth rates.

5.0 SUMMARY OF OBSERVATIONS AND CONCLUSIONS

(I) The examination of P/T samples removed from Pickering NGS A reactors indicates the following:

(a) The internal surface of the P/Ts is covered with a homogeneous one-layer ZrO_2 scale, that shows excellent adherence at the metal/oxide interface.

(b) Scale spallation at the scale/coolant interface due to parallel crack formation was a general characteristic observed in all examined samples. The oxide scales on Zr-2.5 Nb have a more pronounced tendency to spall than those on Zr-2 P/Ts. The scale spallation on Zr-2.5 Nb P/Ts could have an impact on the reliability of information obtained by examination of P/Ts

removed from operating reactors; it may impair our ability to determine the real oxide thickness and establish relationships between corrosion rate, neutron flux and temperature along the fuel channels.

(c) A technique for SEM examination of the P/T oxides was developed. This examination shows that the bulk of the oxide has a granular microstructure consisting of fine equiaxed grains with interconnected porosity.

(II) Out-reactor scale with thickness ranging between 2 and 36 μm were successfully prepared on P/T materials that are used in CANDU reactors (Zr-2.5 Nb β-quenched, Zr-2.5 Nb non-β-quenched and Zr-2) by exposure to LiOH solutions with concentrations ranging between 0.5 and 10 g/L at 300 to 360°C.

(III) The examination of out-reactor scales shows the following:

(a) Under all investigated experimental conditions the out-reactor scales consisted of a homogeneous one-layer oxide with an excellent adherence at the metal/oxide interface. The scales show the same general tendency to spall near the outer scale surface. This tendency was higher for scales on Zr-2.5 Nb than Zr-2. The microstructure of oxide scale on Zr-2.5 Nb samples consists of fine equiaxed grains with interconnected porosity.

(b) Increasing LiOH concentration and/or exposure time appears to enhance the development of scale porosity. At concentrations higher than 4 g/L LiOH the scales lose their compactness and integrity and become powdery.

(c) The Zr-2.5 Nb non-β-quenched materials corrode faster and form less compact and protective scales than Zr-2.5 Nb β-quenched material.

(d) The out-reactor scale formed in steam at CRNL at 490°C was 32 μm thick. The scale showed a tendency to detach at the metal/oxide interface. This more compact scale consists of long columnar grains. The hydrides are significantly larger and denser than in the in-reactor samples.

(IV) The results of the present investigations indicate that both in-and out-reactor scales on pressure tube materials show a tendency to spall-off. Some of the factors influencing this tendency were identified: type of alloy,

sample thermal and metallurgical history, exposure or operating time (thickness) and environmental conditions. Therefore when the scale reaches a certain thickness, not yet identified, it may be impossible to estimate the material corrosion behaviour based only on oxide thickness evaluation.

(V) Comparison of in- and out-reactor scales indicates that oxide scales up to 20 μm in thickness that simulate the morphology of in-reactor scales and display overall integrity similar to in-reactor oxides, could be prepared on Zr-2.5 Nb materials by short-term exposure to 2.5 g/L LiOH solution or long-term exposure to 0.5 g/L LiOH solution at 340°C. Investigations to compare the chemical composition of in-reactor vs out-reactor scales has not been carried out. However general experience suggests that simulations performed by growing oxides in LiOH solutions (used in-reactor at lower concentrations for PHTS pH adjustment) should result in similar, basic characteristics.

6.0 RECOMMENDATION FOR FUTURE WORK

Based on the findings of the present investigation it is recommended that the following future work be performed:

(I) As part of this program, a SEM technique was developed for in-reactor scale examination. It is proposed to continue to use this technique to assess the oxide scales on the internal surface of P/Ts that are removed periodically from CANDU reactors.

(II) To reduce the pre-oxidation time required to grow thick oxides, higher temperature tests should be carried out in 0.5 g/L LiOH solution.

(III) To compare the characteristics of in- and out-reactor scales, tests to evaluate their memory effect should continue.

(IV) Development of improved technique capability for characterization of oxides on P/Ts and evaluation of oxides spalling effects on P/T corrosion and hydriding behaviour is needed.

(a) TEM techniques to examine the detailed microstructure of oxide scale (pore size and distribution, grain shape and size, crack network and surface defects) and base alloy at the metal/oxide interface.

(b) Surface analysis techniques (EDX, ESCA, SIMS) to establish the elemental and phase composition of

scales and detect elements such as Li and Nb, and their distribution in ZrO_2 and at the metal/oxide interface.

(c) Irradiated oxide porosity measurement techniques.

7.0 ACKNOWLEDGEMENTS

The funding for this project was provided by Nuclear Materials Management Dept, Design and Development Division. This support is gratefully acknowledged. Messrs. J.S. Li, R.E. Heathcock and especially Mrs. E.G. Csillag of this department are thanked for their permanent encouragement to pursue the ideas of this work.

Experimental work has been carried out by technical staff from OHRD and AECL. Special thanks to Mr. E. Rasile, Mrs. S. Sandloeken, Mr. L.G. Woodworth, Mr. F.W. Stanley and Mr. A. Shaddick.

Useful discussions with Dr. P.C. Lichtenberger from OHRD and Dr. B. Cox and Mr. V. Urbanic from CRNL are greatly appreciated. Last, but certainly not least, the author is grateful to Drs. C.J. Simpson and P. Mayer for helpful comments on the experimental program and report.

Approved by:

James Brown

J. Brown
Manager
Metallurgical Research Dept

Prepared by:

A. Manolescu

A.V. Manolescu
Engineer - Corrosion
Corrosion & Tritium
Technology Section
Metallurgical Research Dept

Reviewed by:

P.C. Lichtenberger

P.C. Lichtenberger
Supervising Scientist
Corrosion & Tritium
Technology Section
Metallurgical Research Dept

AVM:em/lg

REFERENCES

1. B. Cox, P.C. Lichtenberger and V.F. Urbanic, "Fuel Channel Corrosion Programs", CRNL-2708-20, July 1986.

2. A. Shaddick, C.K. Chow, L.G. Woodworth and F.W. Stanley, "Oxide Morphology of Pickering Pressure Tubes P1-K18, P3-J09 and P4-N16", Atomic Energy of Canada Ltd., Report CRNL-2933, March 1986.

3. A.V. Manolescu, "Fuel Channel Out-Reactor Corrosion Under Simulated Conditions (FOCUS) Program", Quarterly Progress Report, Ontario Hydro Research Division, January 20, 1986.

4. D. Rogers, V. Urbanic and E.F. Ibrahim "The Examination of the Cold Worked Zr-2.5 wt% Nb Pressure Tube from Pickering Unit 4 Fuel Channel N16", CRNL - 2597-15, August 1985.

5. A.B. Johnson, Jr, "An Assessment of Corrosion and Hydriding on Zircoloy-2 Pressure Tubes from Pickering Units 1 and 2", BN-SA-2153, September 1984.

6. D.H. Broadhurst and P.A. Heuer, J. Nucl. Mater. 37 (1970), 35.

7. B. Cox, J. Nucl. Mater. 27 (1968) 1.

8. B. Cox, J. Nucl. Mater. 29 (1969) 50.

9. B. Cox and A. Donner, J. Nucl. Mater. 47 (1973) 72.

10. A.B. Johnson, Jr., Proc. of 4th Intl. Cong. on Metallic Corrosion, Amsterdam 1969, 168.

11. B. Cox, "The Morphology of Zirconium Films and its Relation to the Oxidation Kinetics", AECL Report-3285, 1969.

12. A.V. Manolescu, E.M. Rasile and P. Mayer, "Crevice Corrosion Between Pressure Tubes and Fuel Bundles Bearing Pads, Proceedings of Fuel Channel Technology Seminar", Oakville, Ontario, November 1985.

13. C. Roy and G. David, J. of Nucl. Mater. 37, (1970) 71.

14. B. Cox, J. of Australian Inst. of Metals, 14 (1969) 123.

15. A.W. Urquhart and D.A. Vermilyea, "Characterization of Zircaloy Oxidation Films", Zirconium in Nuclear Applications, ASTM STP 551 (1974) 463.

16. G.P. Sabol, S.G. McDonald and G.P. Airey, "Microstructure of the Oxide Films Formed on Zirconium Based Alloys", Zirconium in Nuclear Applications, ASTM STP 551, (1974) 435.

17. A.V. Manolescu, P. Mayer and C.J. Simpson, Corrosion, 38 (1982) 23.

Table I

DESCRIPTION OF EXAMINED P/T

Reactor/ Unit	P/T Identi-fication	Type of P/T material	Reactor Operating History (EFPH*)	Internal Surface Finish of P/T Before Installation In-Reactor
PNGS A 3	P3-J09	Zr-2.5 Nb Non β-quenched	83670	cold worked sandblasted, caustic washed and autoclaved
PNGS A 4	P4-N16	Zr-2.5 Nb Non β-quenched	82370	cold worked sandblasted, caustic washed and autoclaved
PNGS A 1	P1-K-18	Zr-2	88900	cold worked pickled and autoclaved

*Equivalent Full Power Hours

Table II

LOCATION OF STUDIED P/T SAMPLES*

P/T Identification	Sample Location		Techniques Used for Examinations
	Distance from Inlet (cm)	In-Reactor Clock Position	
P3-J09	115.7-119.7	1	OM, SEM
	347.9-351.9	1	OM, SEM
	476.9-484.9	1	SEM
	487.3-491.3	1	OM
P4-N16	60.9-64.9	1	OM, SEM
	289.6-293.6	1	OM, SEM
	569.4-573.4	1	OM, SEM
	569.4-573.4	5	OM, SEM
P1-K18	39.2-42.2	12	OM
	345.1-348.1	12	OM
	592.5-595.5	12	OM

*Selection of sample location was based on P/T sample availability.

Table III

CORROSION TESTS IN LiOH SOLUTIONS;
EXPERIMENTAL PARAMETERS

Type of P/T Material	Zr-2.5 Nb β-quenched Zr-2.5 Nb non-β-quenched Zr-2
Concentration of LiOH Solution (g/L)	0.1 0.5 1.0 2.5 4.0 10.0
Temperature (°C)	300 340 360 380
Exposure (days)	2 - 40

Table IV

CONCENTRATION OF LiOH IN TEST SOLUTIONS

LiOH Concentration (g/L)	Molarity (M)	Measured pH at RT	Theoretical pH at RT
0.5	0.02	11.4	12.3
1.0	0.042	11.9	12.6
2.5	0.104	12.1	13.0
4.0	0.16	12.3	13.2
10.0	0.418	12.3	13.6
23.9 /17/	1.00	12.5	14.0

Table V

MAXIMUM THICKNESS OF OXIDE SCALES ON P3-J09 P/T

Sample Location (cm From Inlet)	Clock Position	Maximum Thickness of Oxide Scale (μm)
115.7-119.7	1	13
347.9-351.9	1	14
476.9-484.9	1	16

Table VI

MAXIMUM THICKNESS OF OXIDE SCALES ON P4-N16 P/T

Sample Location (cm From Inlet)	Clock Position	Maximum Thickness of Oxide Scale (μm)
60.9-64.9	1	10
289.6-303.6	1	12
569.6-573.4	1	13
569.7-573.7	5	13

Table VII

MAXIMUM THICKNESS OF OXIDE SCALES ON P1-K18 P/T

Sample Location (cm From Inlet)	Clock Position	Maximum Thickness (μm)
39.2-42.2	10	32
345.1-348.1	12	36
592.5-595.5	10	52

TABLE VIII - RESULTS OF CORROSION TESTS* IN LiOH SOLUTIONS

Test Description			Results		Scale Thickness (μm)			
					Zr-2.5 Nb β-q		Zr-2.5Nb non-β-q	
c (g/L)	T (°C)	t (Days)	Scale Appearance on Zr-2.5 Nb	Scale Morphology on Zr-2.5 Nb	Calc. **	Meas-ured	Calc. **	Measured
10	300	6	uniform white, powdery scale	one-layer oxide scale; it spalls close to Me/oxide interface; a loose and flaky scale	3.7	-	6.1	-
4	340	2	uniform white, powdery scale	one-layer scale; the scale is adherent at Me/oxide interface and spalling at oxide/water interface; compact scale on Zr-2.5 Nb β-quenched	9.2	13	10.1	17
4	340	6	uniform white, powdery scale	one-layer scale, adherent at Me/oxide interface, severely spalling at the outer interface	29	34	32.7	42
2.5	340	6	uniform white, hard compact scale	one-layer oxide scale; cracks parallel with Me/oxide interface especially on Zr-2.5Nb non-β-quenched.	18	20	20	26
2.5	340	9	uniform white, powdery oxide	one-layer scale; adherent at Me/oxide interface. Because of a large number of parallel cracks the scale appears loose and flaky	28.6	36	29.7	37
1	340	11	uniform white and powdery scale	one-layer scale adherent scale at Me/oxide interface, spalls at outer interface, loose scale	14	19	16	23
2.5	300	16	uniform white, loose scale	the scale spalls very close to metal/oxide interface; a loose and flaky scale	7.9	-	8.1	-
0.5	340	40	mixture of dark grey and white oxide hard and compact	homogeneous one oxide layer, adherent at Me/oxide interface spalling at oxide/water interface, compact	3.7	4.0	4.1	4.8
0.5	360	22	same as above	same as above	1.5	2.0	1.6	3.1

* Tests are listed in chronological order.
** Oxide thickness was calculated from the weight gain using formula 14.6 mg/dm^2 = 1.0 μm

Table IX

SURFACE AREA OF OUT REACTOR OXIDE SCALES

Type of P/T Material	Test Conditions			Surface Area (m^2/g)
	Conc of LiOH (g/L)	T (°C)	Time (days)	
Zr-2.5 Nb β-quenched*	4	360	6	22
Zr-2.5 Nb β-quenched*	24	340	1	48
Zr-2.5 Nb β-quenched	Steam	490	60	2
Zr-2*	24	340	2	7

*Samples from previous work/17/.

Table X

COMPARISON OF CALCULATED AND MEASURED AVERAGE SCALE THICKNESS

Type of P/T Material	Test Description			Calculated Thickness (μm)	Measured Thickness (μm)	Approximate Scale Porosity %
	C (g/L)	T (°C)	Time (days)			
Zr-2.5 Nb β-q*	0.01	300	60	1.8	2.0	10.0
Zr-2.5 Nb non-β-q*	0.01	300	60	2.0	2.3	13.0
Zr-2.5 Nb β-q	0.5	340	40	3.7	4.0	7.5
Zr-2.5 Nb non-β-q	0.5	340	40	4.1	4.8	14.5
Zr-2.5 Nb β-q	2.5	340	6	18	22	18.0
Zr-2.5 Nb non-β-q	2.5	340	6	20	26	23.0
Zr-2.5 Nb β-q	steam	490	60	32	33	3.0

*Samples from FOCUS program, Ref /3/.
q = quenched

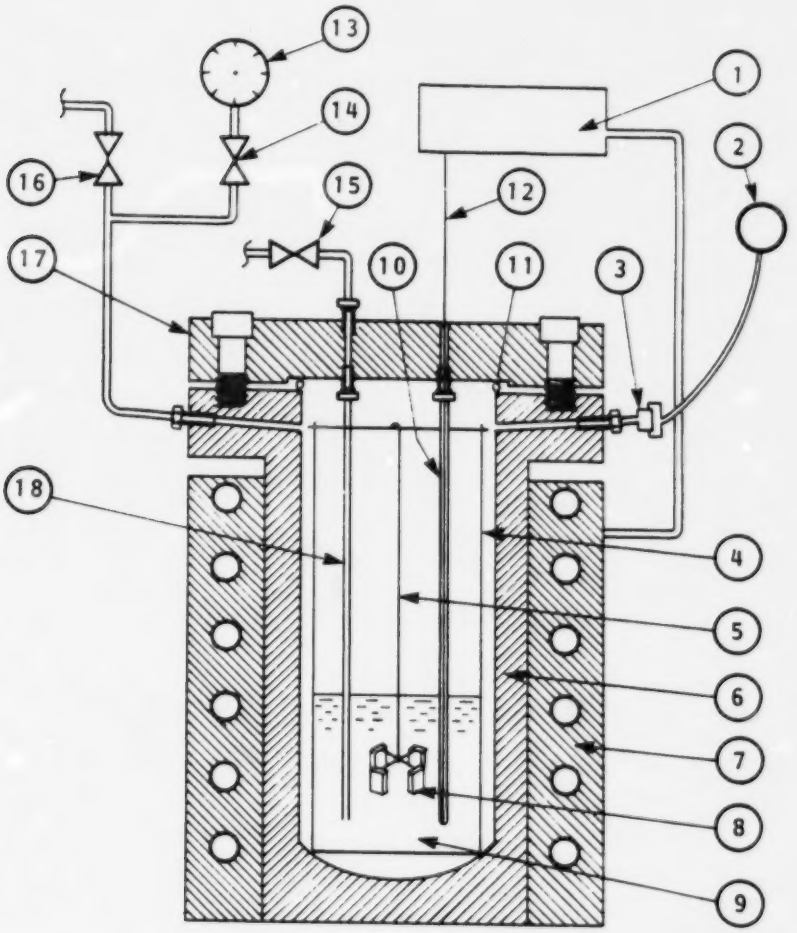

1 FURNACE CONTROLLER
2 STEAM TRAP
3 RUPTURE DISC ASSEMBLY
4 NICKEL LINER
5 Zr-2 WIRE
6 VESSEL
7 FURNACE
8 TEST SAMPLE
9 TEST SOLUTION
10 THERMOWELL
11 SEAL RING
12 THERMOCOUPLE
13 PRESSURE GAUGE
14 PRESSURE GAUGE ISOLATION VALVE
15 PURGING SHUT OFF VALVE
16 PRESSURE RELEASE VALVE
17 AUTOCLAVE HEAD ASSEMBLY
18 PURGING TUBE

FIGURE 1
SCHEMATIC OF THE AUTOCLAVE TEST ASSEMBLY

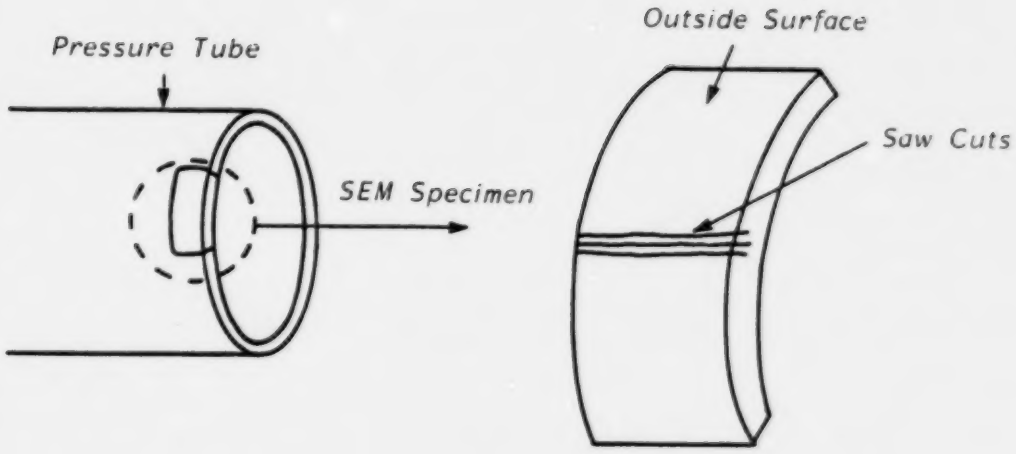

FIGURE 2

SCHEMATIC OF P/T SAMPLES USED
FOR SEM EXAMINATION /2/

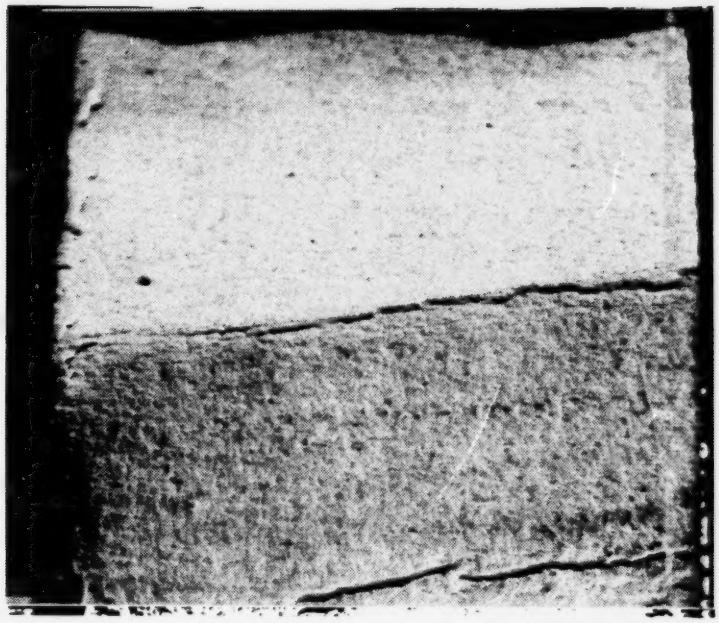

FIGURE 3

TYPICAL P/T SAMPLE AFTER BENDING FOR
EXAMINATION UNDER THE SEM
(P4-N16 P/T SAMPLE 60.9-67.9cm FROM INLET)

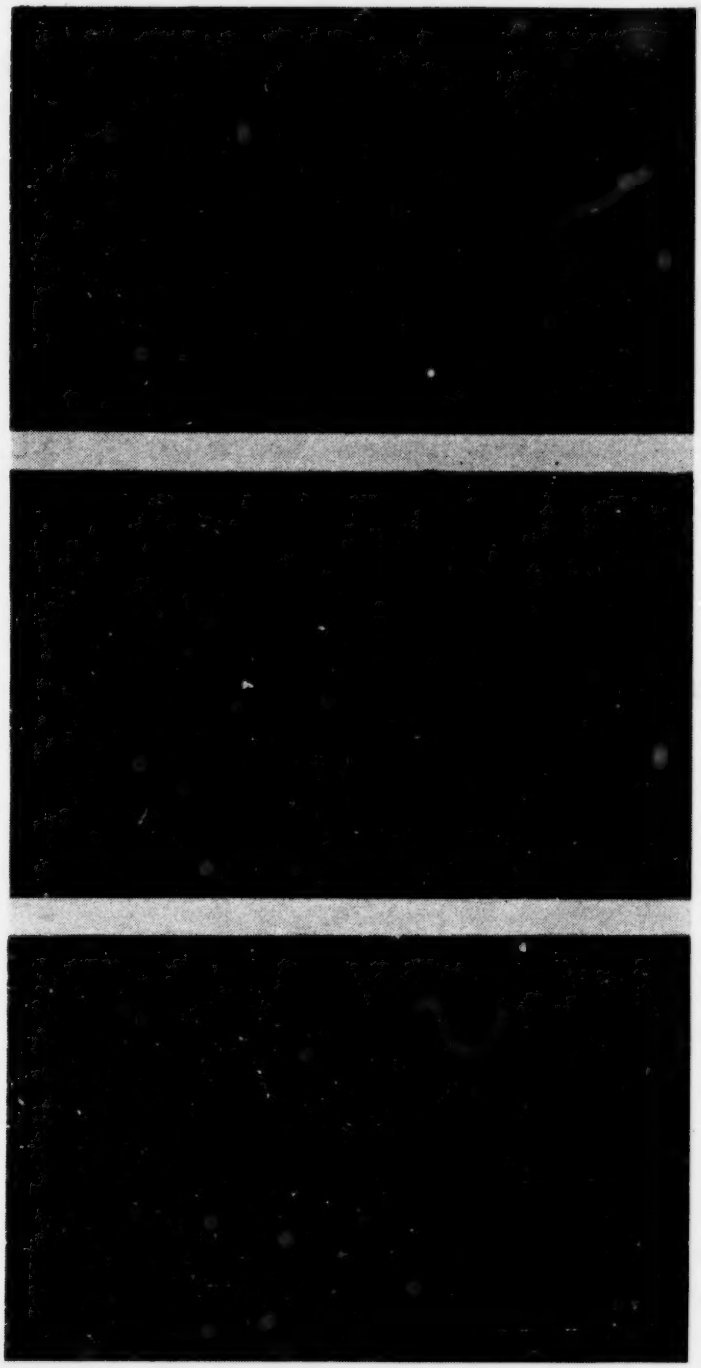

115.7-119.7cm from inlet (1: o'clock)

347.9-359.1cm from inlet (1: o'clock)

471.0-479.7cm from inlet (1: o'clock)

FIGURE 4

INTERNAL SURFACE OF P3-J09 P/T SAMPLES FROM DIFFERENT LOCATIONS (x51)

171784 RD

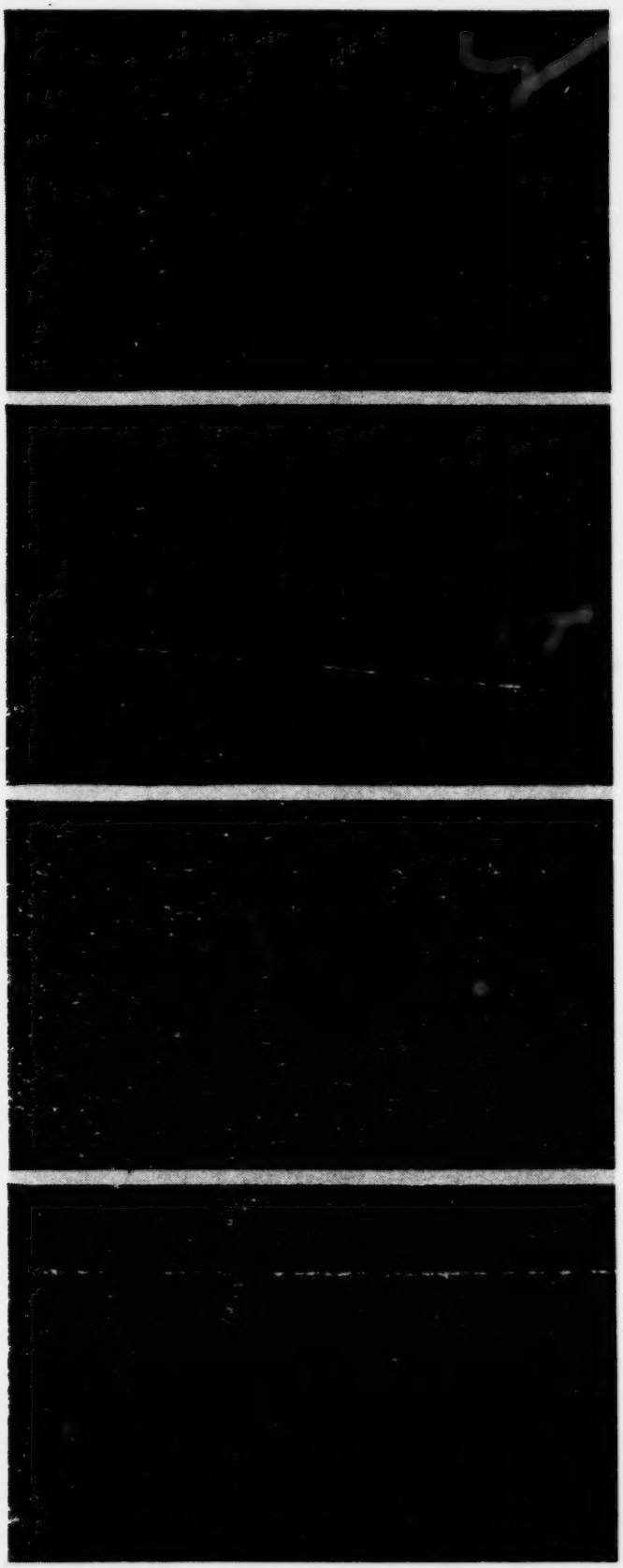

60.9-64.9cm
from inlet
(1: o'clock)

289.6-293.6cm
from inlet
(1: o'clock)

569.4-573.4cm
from inlet
(1: o'clock)

569.4-573.4cm
from inlet
(5: o'clock)

FIGURE 5

INSIDE SURFACE OF P4-N16 P/T SAMPLES
FROM DIFFERENT LOCATIONS (x51)

171785 RD

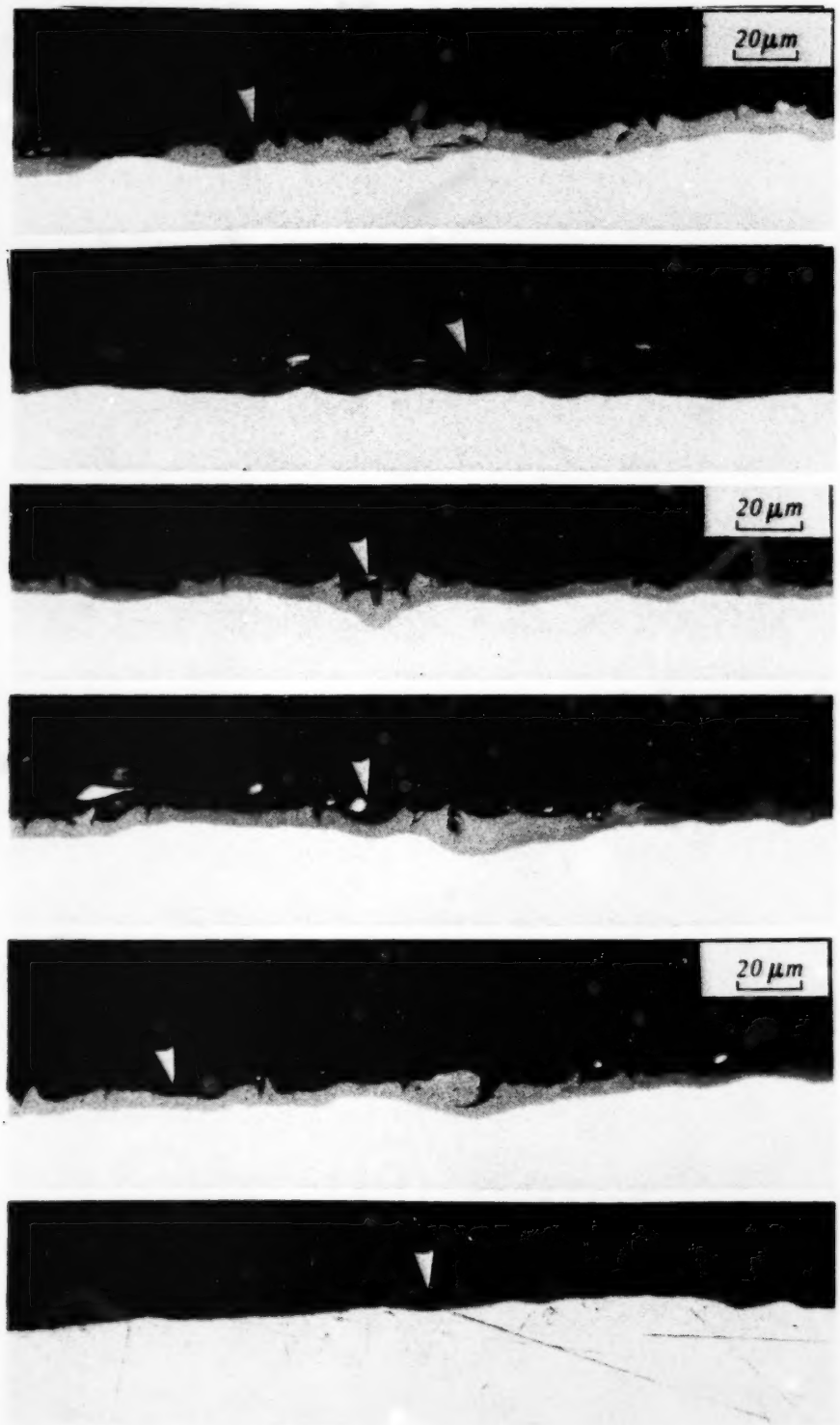

FIGURE 6

TYPICAL CROSS SECTIONS OF OXIDE SCALES ON
INTERNAL SURFACE OF P3-J09 P/T AT DIFFERENT LOCATIONS

171786 RD

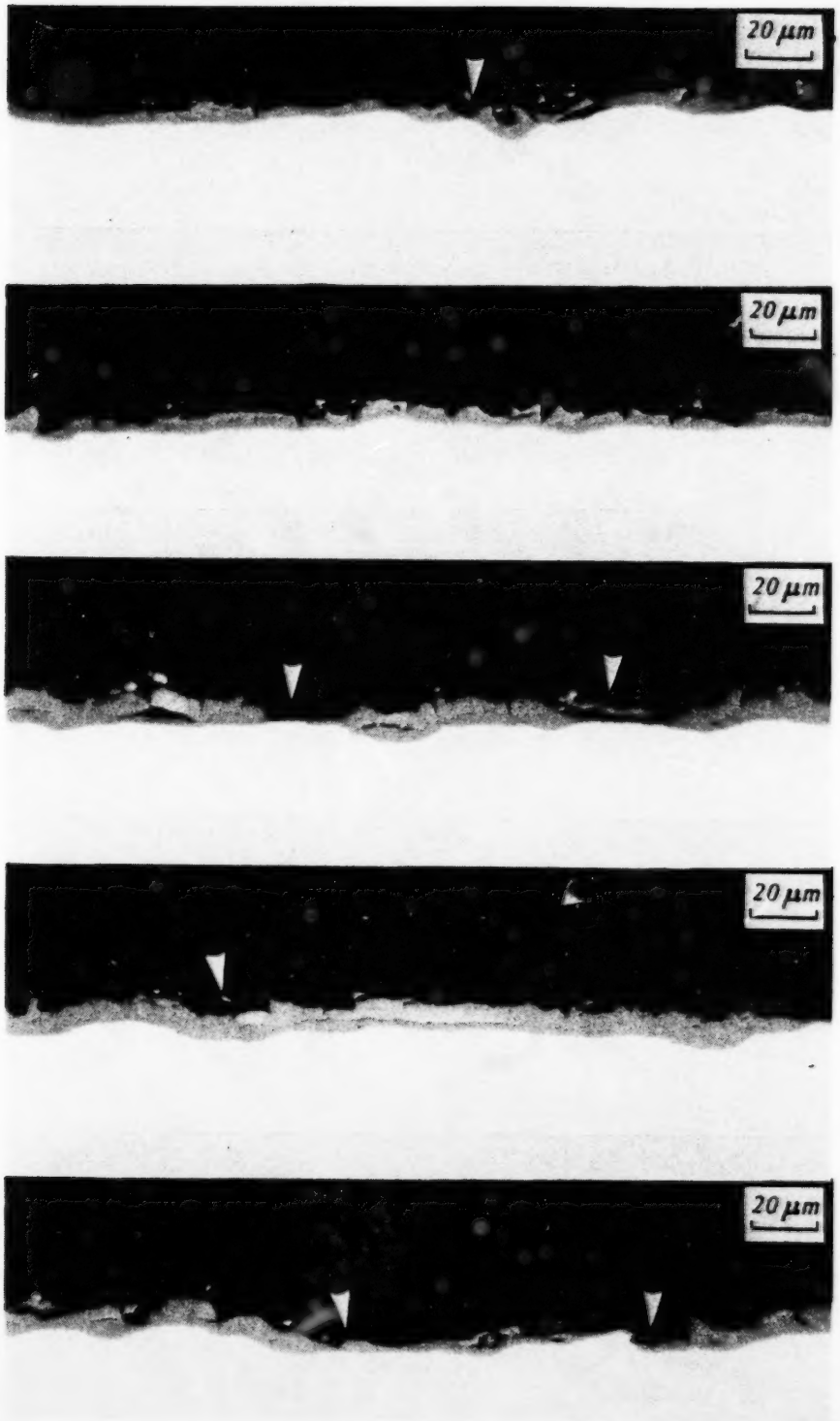

A
60.9-64.9cm
from inlet
(1: o'clock)

B
289.6-393.6cm
from inlet
(1: o'clock position)

C
569.4-573.4cm
from inlet
(1: o'clock porosity)

D
569.4-573.4cm
from inlet
(5: o'clock position)

E
569.4-573.4cm
from inlet
(5: o'clock position)

FIGURE 7

TYPICAL CROSS SECTIONS OF THE OXIDE SCALES
ON P4-N16 P/T AT DIFFERENT LOCATIONS

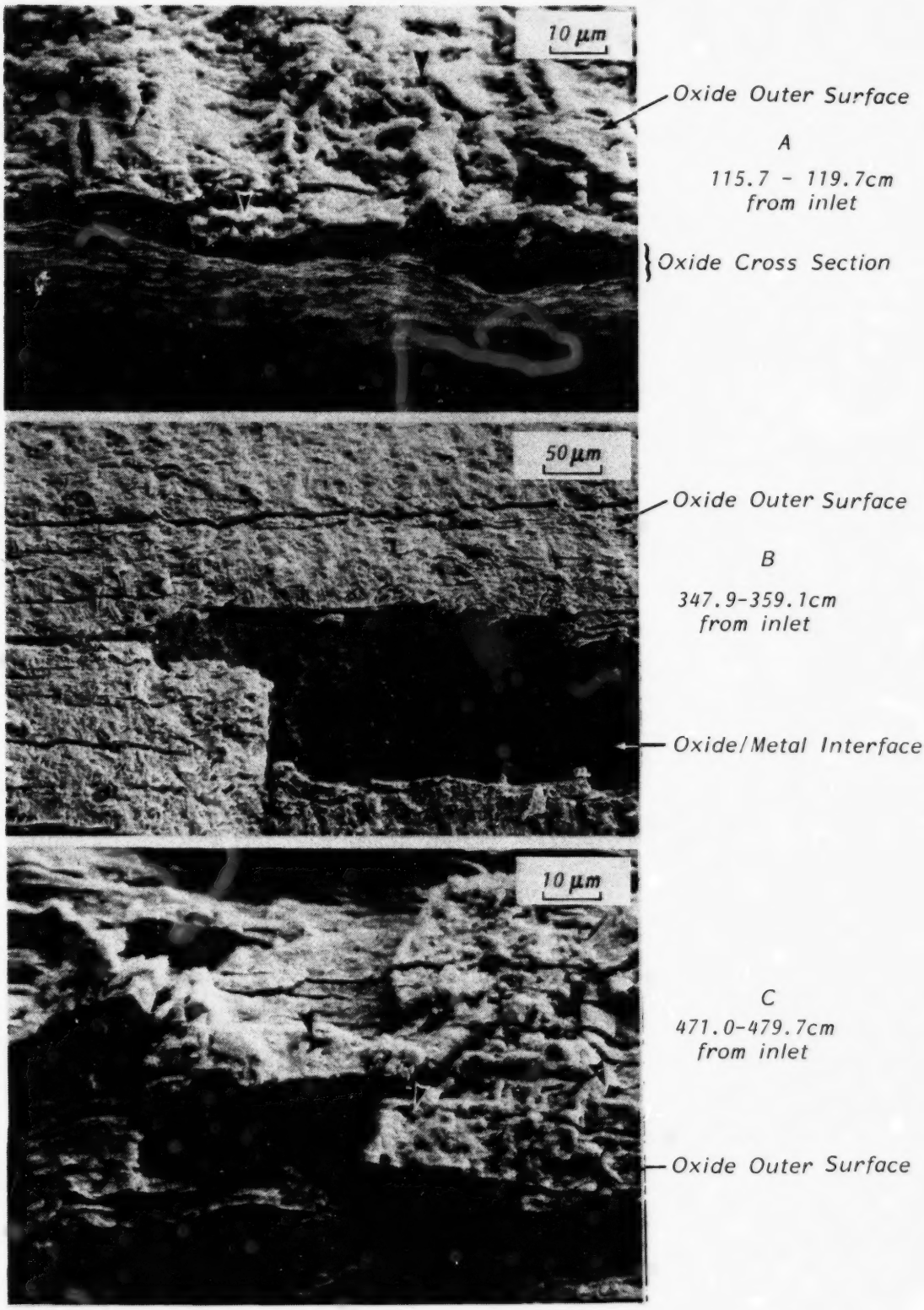

FIGURE 8

TYPICAL LOW MAGNIFICATION SCANNING ELECTRON MICROGRAPHS
OF FRACTURED OXIDE SCALES ON P3-J09 P/T AT DIFFERENT LOCATIONS

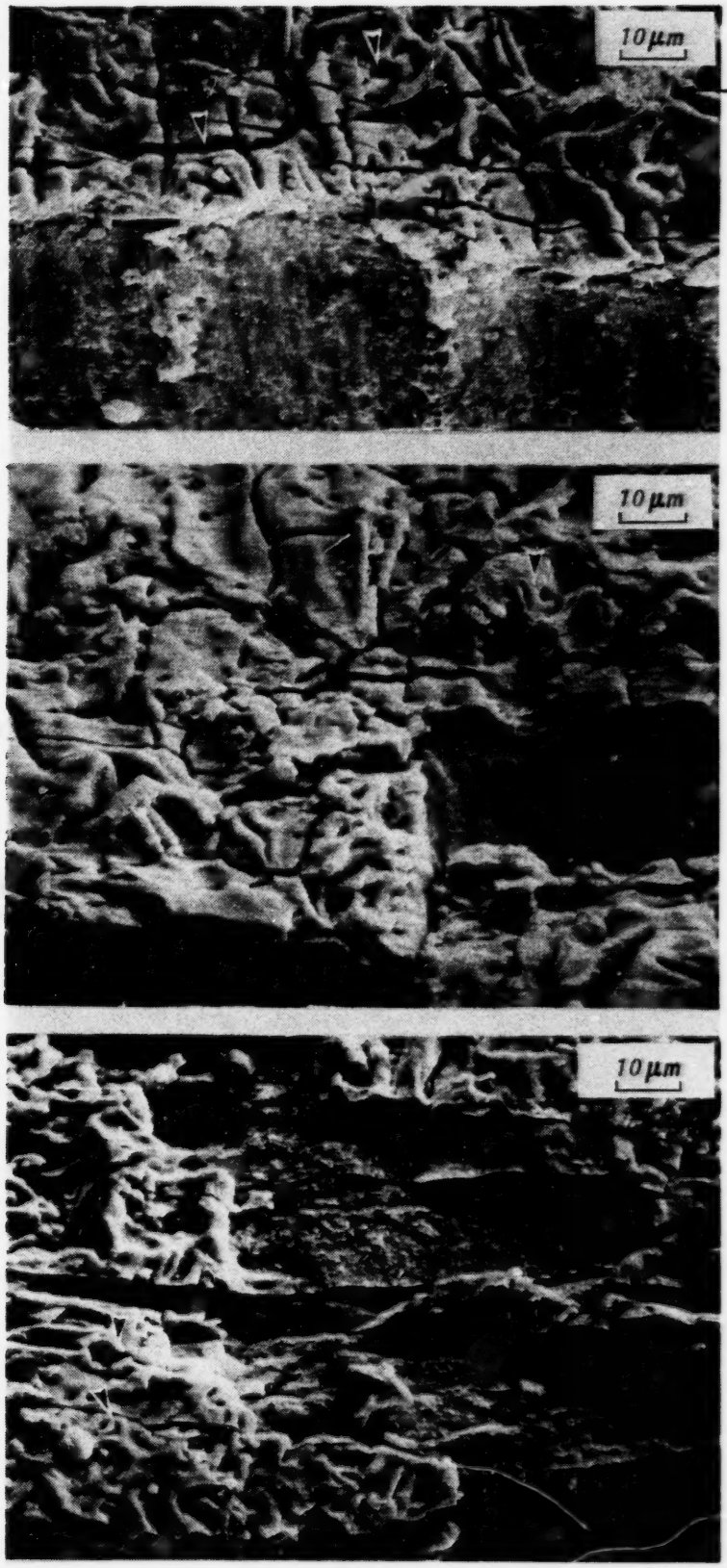

FIGURE 9

TYPICAL LOW MAGNIFICATION SCANNING ELECTRON MICROGRAPHS
OF FRACTURED OXIDE SCALES ON P4-N16 P/T AT DIFFERENT LOCATIONS

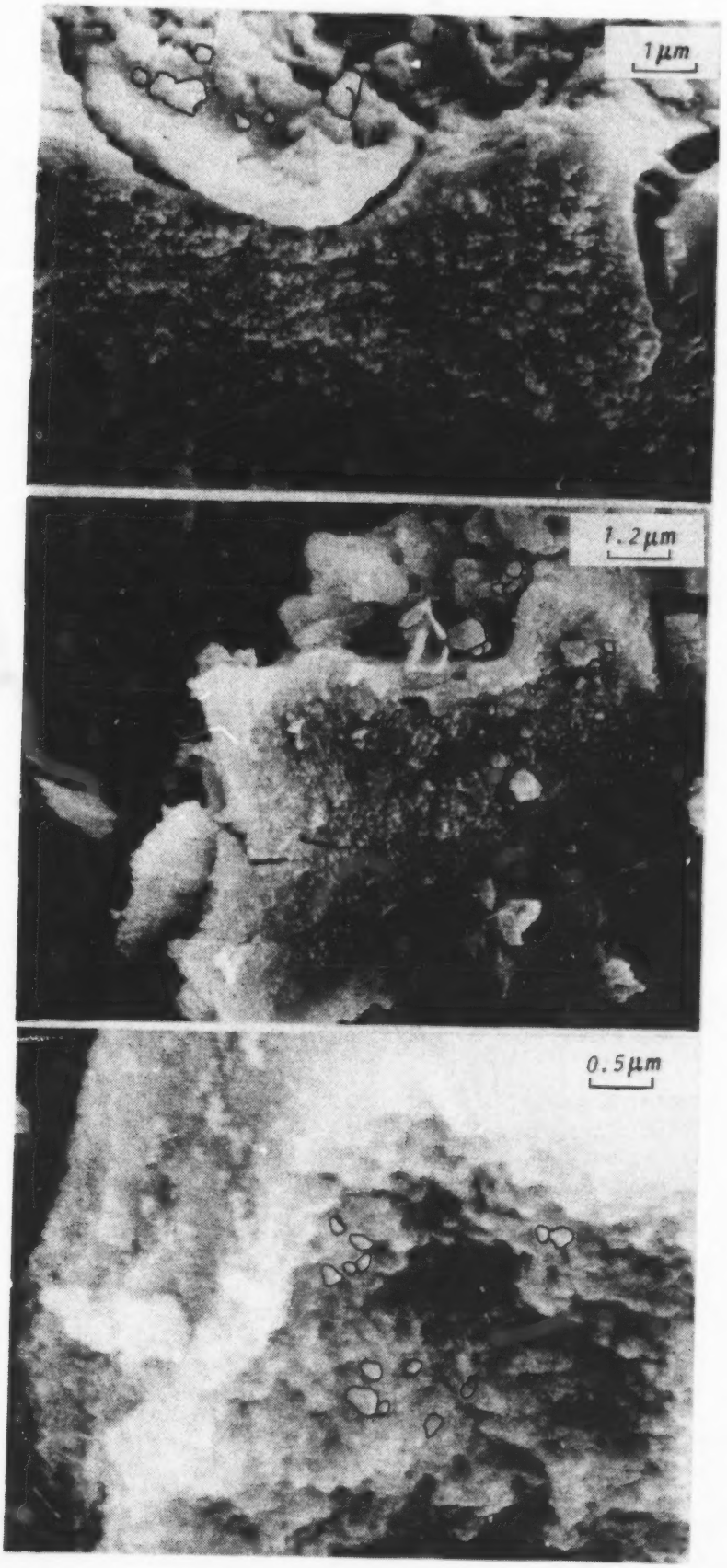

A
115.7-119.7cm
from inlet

B
347.9-359.1cm
from inlet

C
471.0-479.7cm
from inlet

FIGURE 10

CLOSE-UP OF FRACTURED OXIDE SCALE
AT DIFFERENT LOCATIONS ON P3-J09 P/T

171790 RD

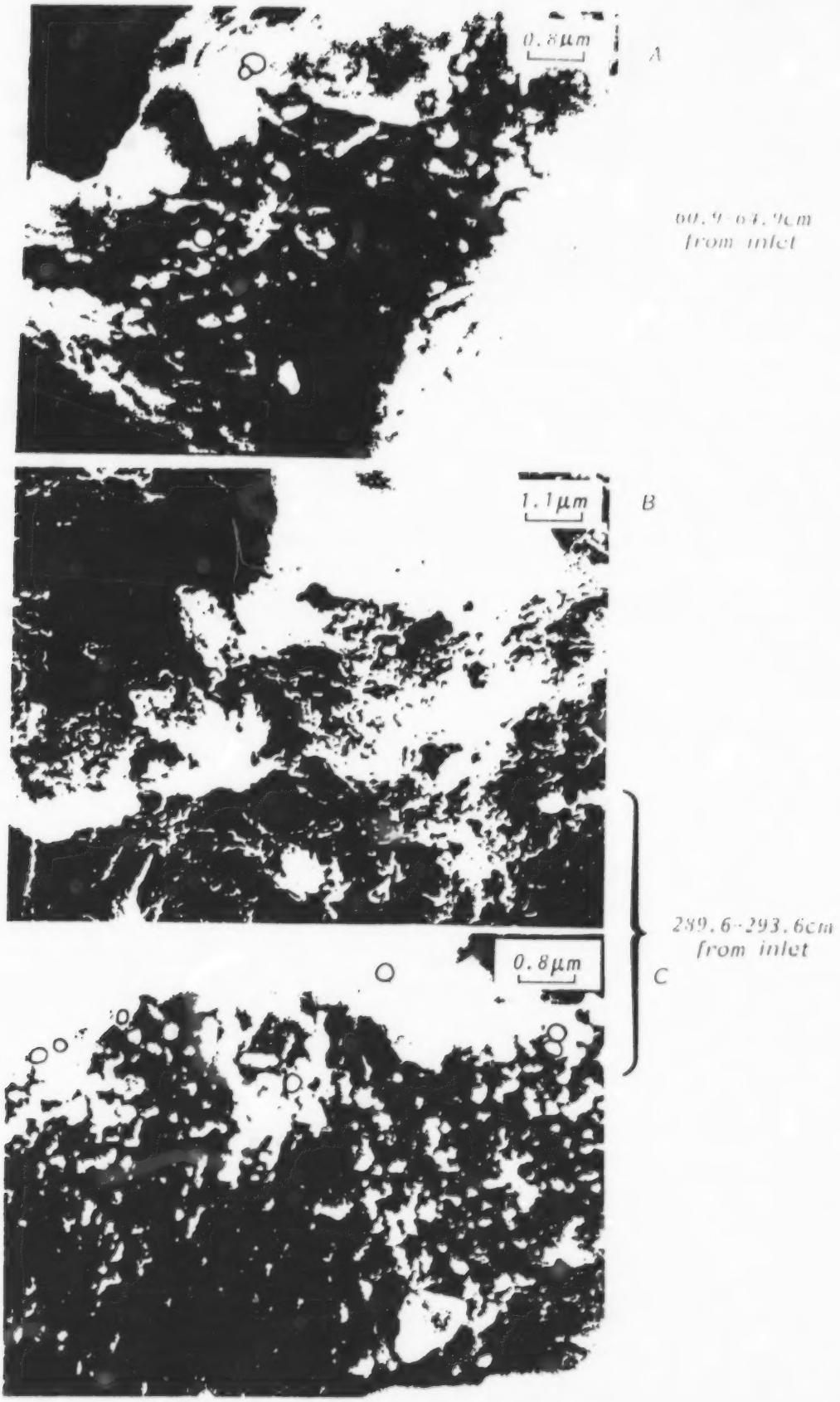

FIGURE 11

CLOSE-UP OF FRACTURED OXIDE SCALE
AT DIFFERENT LOCATIONS ON P4-N16 P/T

D

569.4 - 573.4cm
from inlet
(1: o'clock position)

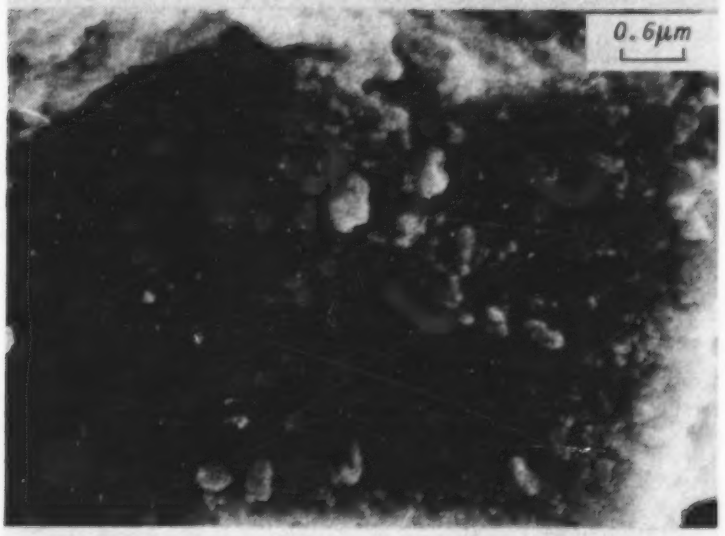

E

569.4 - 573.4cm
from inlet
(1: o'clock position)

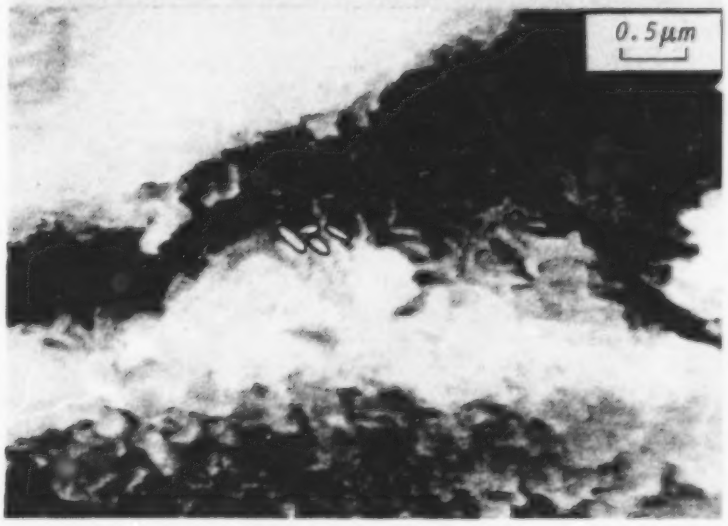

F

569.4 - 573.4cm
from inlet
(5: o'clock position)

FIGURE 11 (CONTINUED)

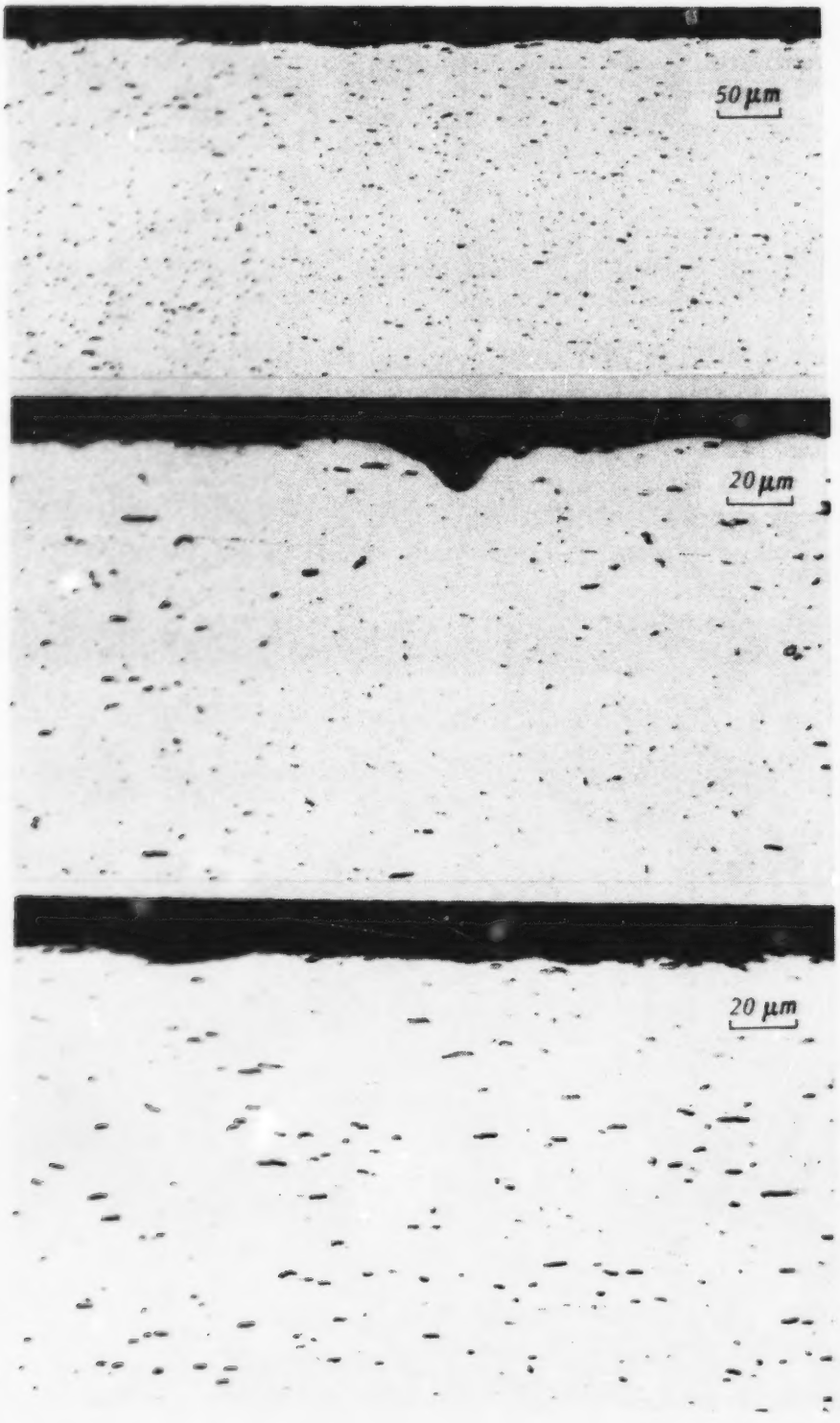

FIGURE 12

TYPICAL HYDRIDE STRUCTURE UNDER THE OXIDE SCALE ON THE INTERNAL SURFACE OF P3-J09 P/T AT DIFFERENT LOCATIONS

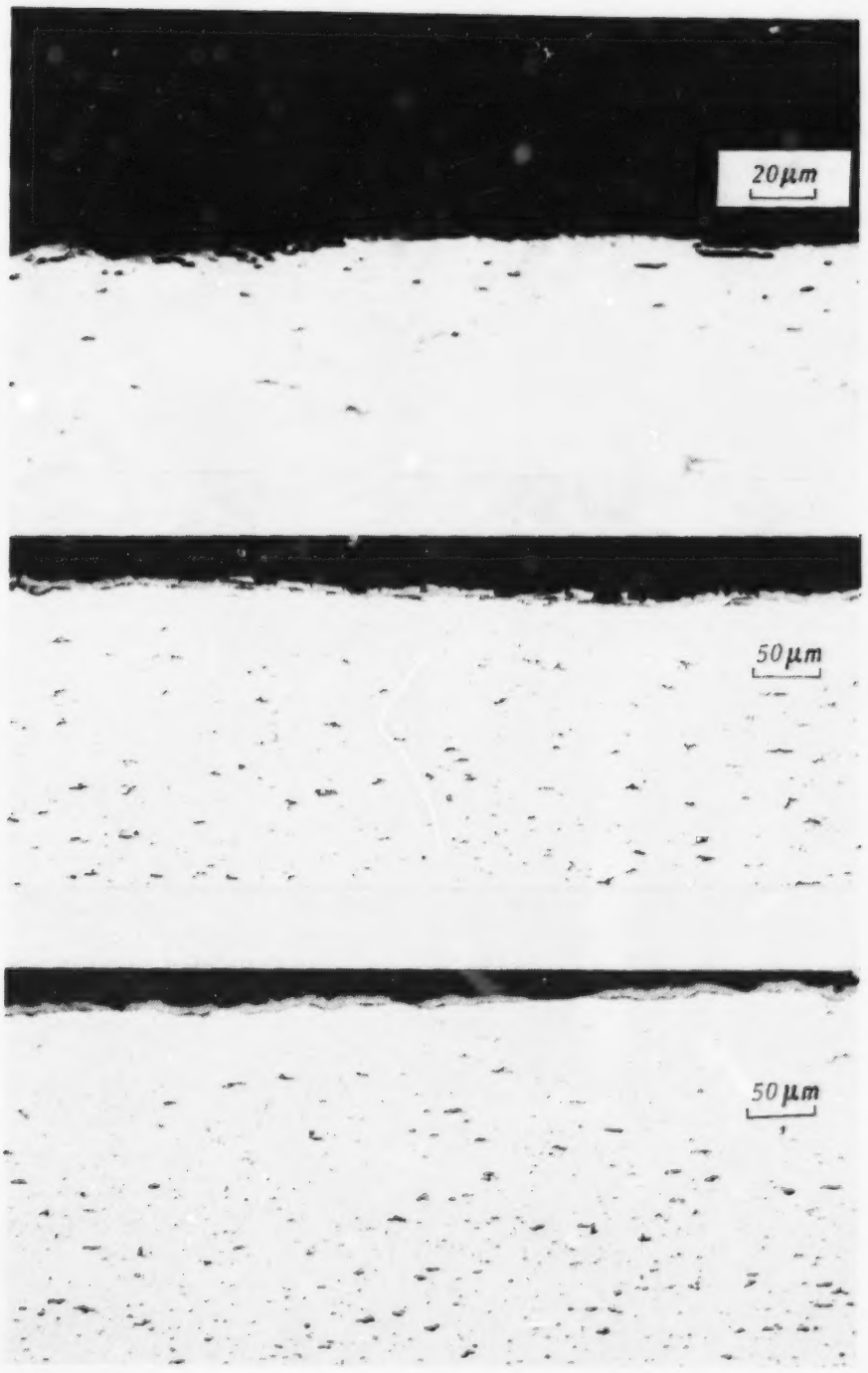

FIGURE 13

TYPICAL HYDRIDE STRUCTURE UNDER THE OXIDE SCALE AT DIFFERENT LOCATIONS ON THE INTERNAL SURFACE OF P4-N16 P/T

171794 RD

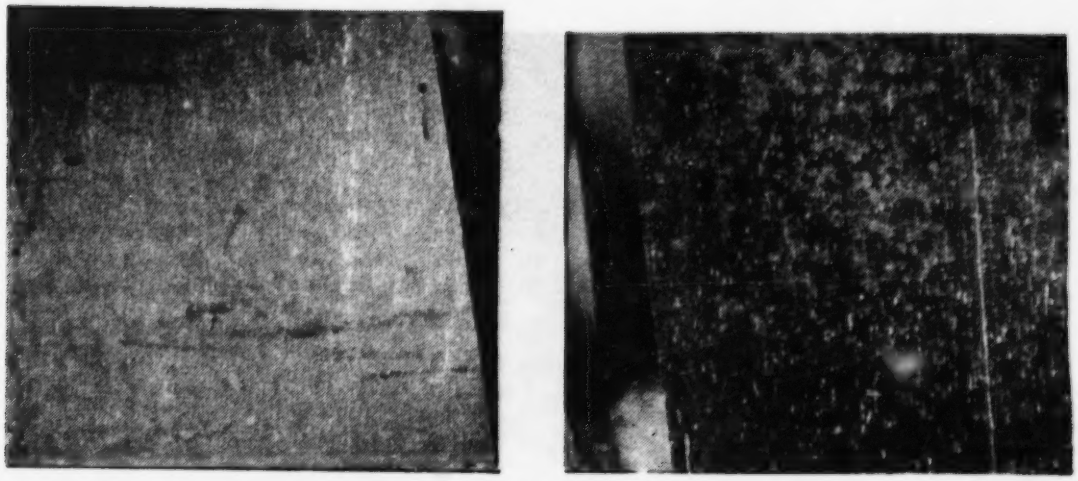

(a) (b)

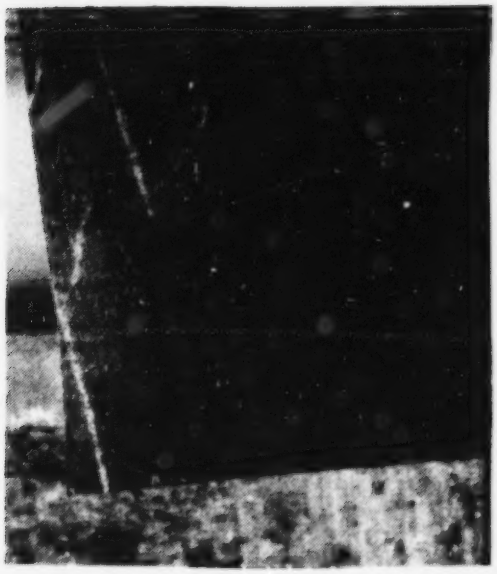

(c)

FIGURE 14

INSIDE SURFACE OF P1-K18 (X 3.3)

(a) 39.2- 42.2cm from inlet
(b) 345.1-348.1cm from inlet
(c) 592.5-595.5cm from inlet

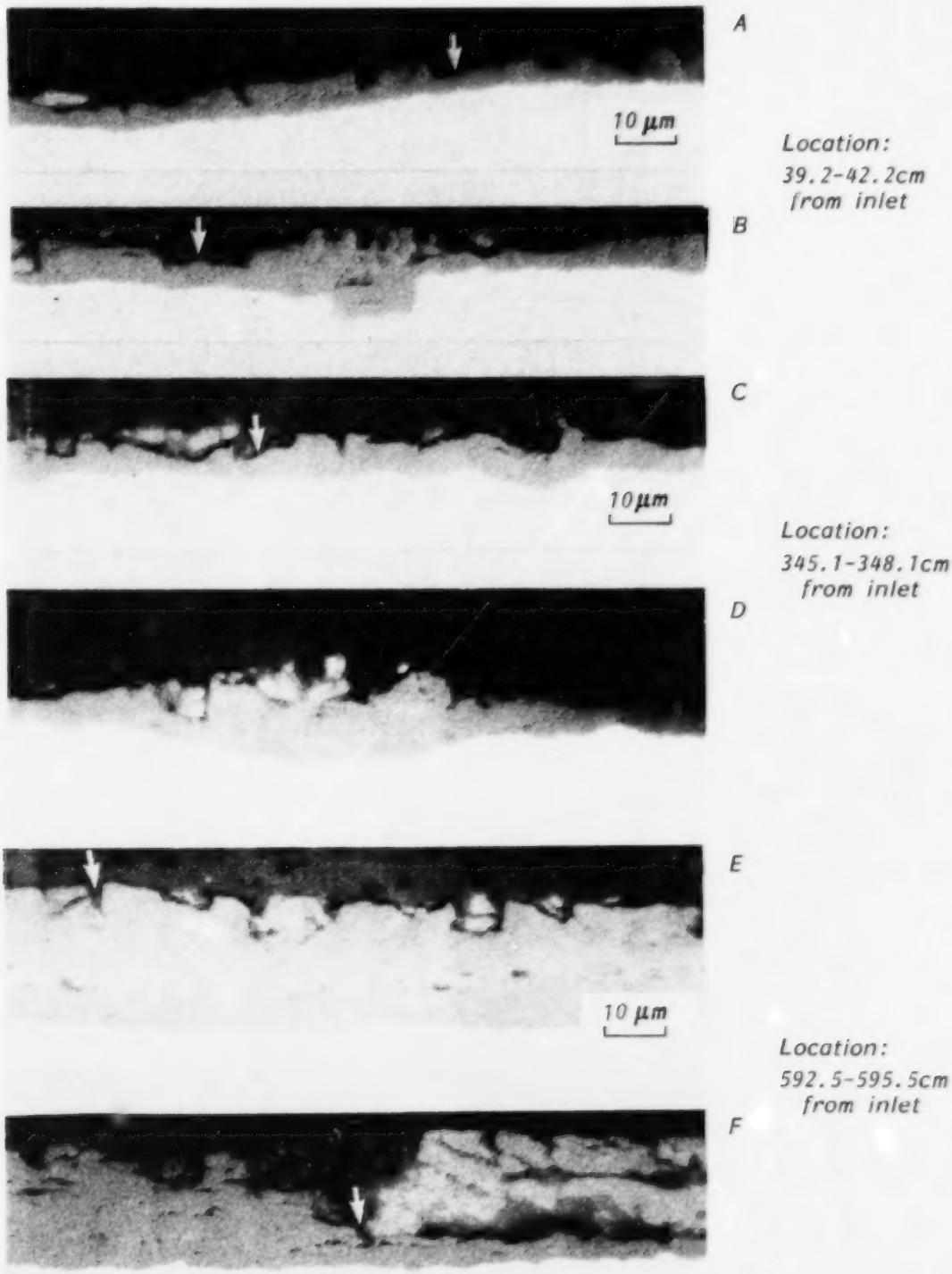

FIGURE 15

TYPICAL CROSS SECTIONS OF OXIDE SCALE ON THE INSIDE SURFACE OF P1-K18 PRESSURE TUBE FROM DIFFERENT LOCATIONS

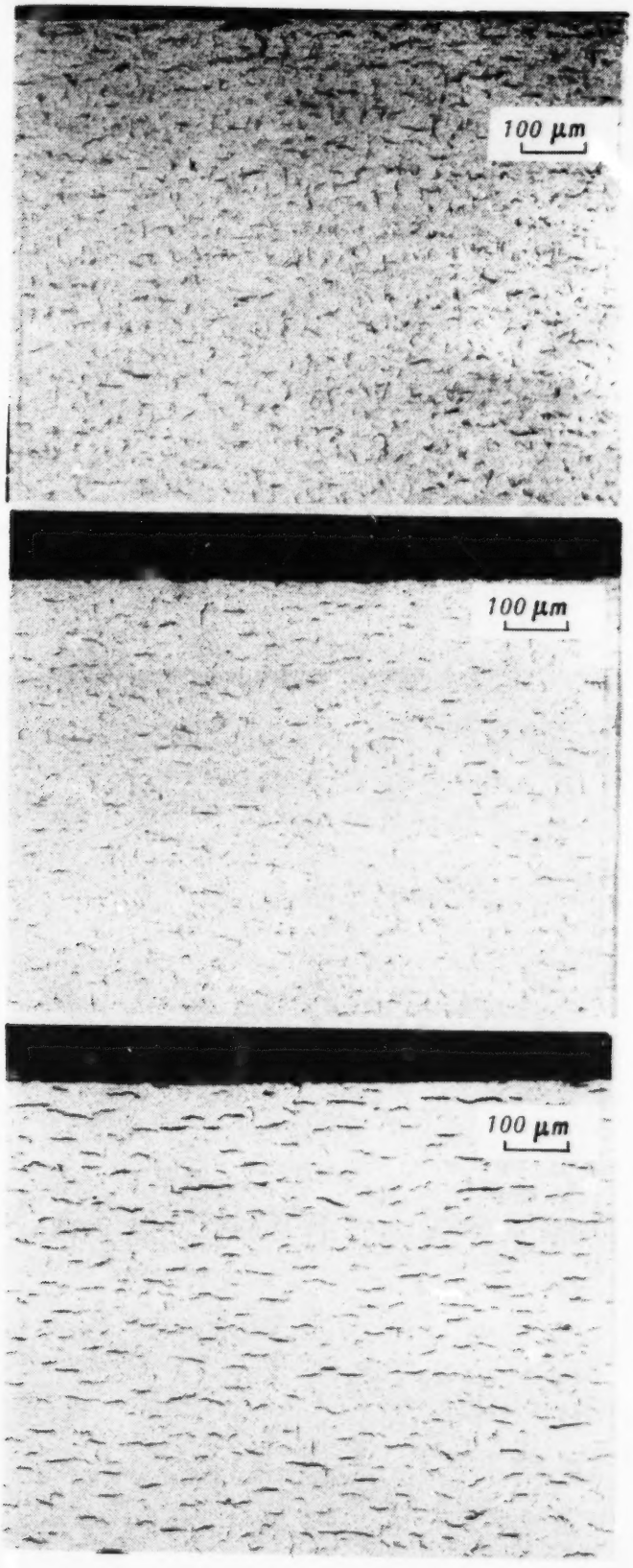

FIGURE 16

TYPICAL HYDRIDE STRUCTURE ON P1-K18
SAMPLES AT DIFFERENT LOCATIONS ON P/T

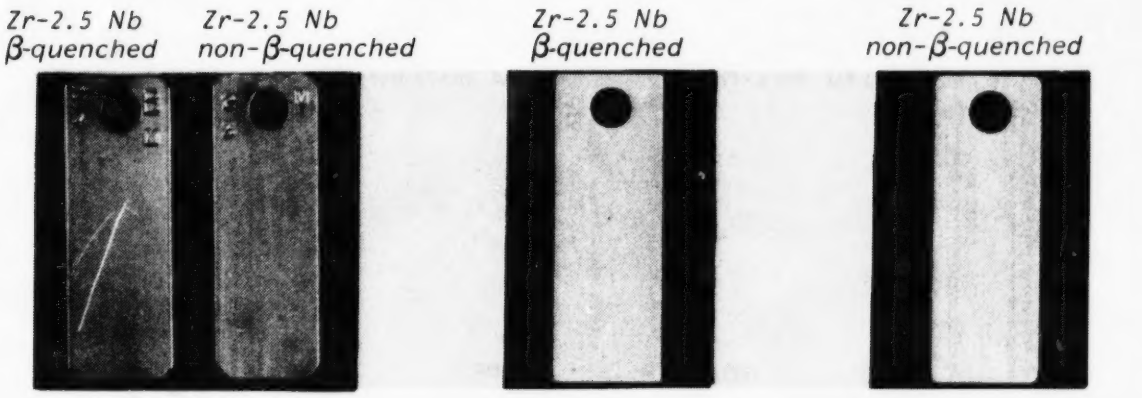

FIGURE 17

TYPICAL CONDITION OF THE OXIDE SCALE ON THE INTERNAL SURFACE OF THE P/T CORROSION SAMPLES AFTER CORROSION TESTS

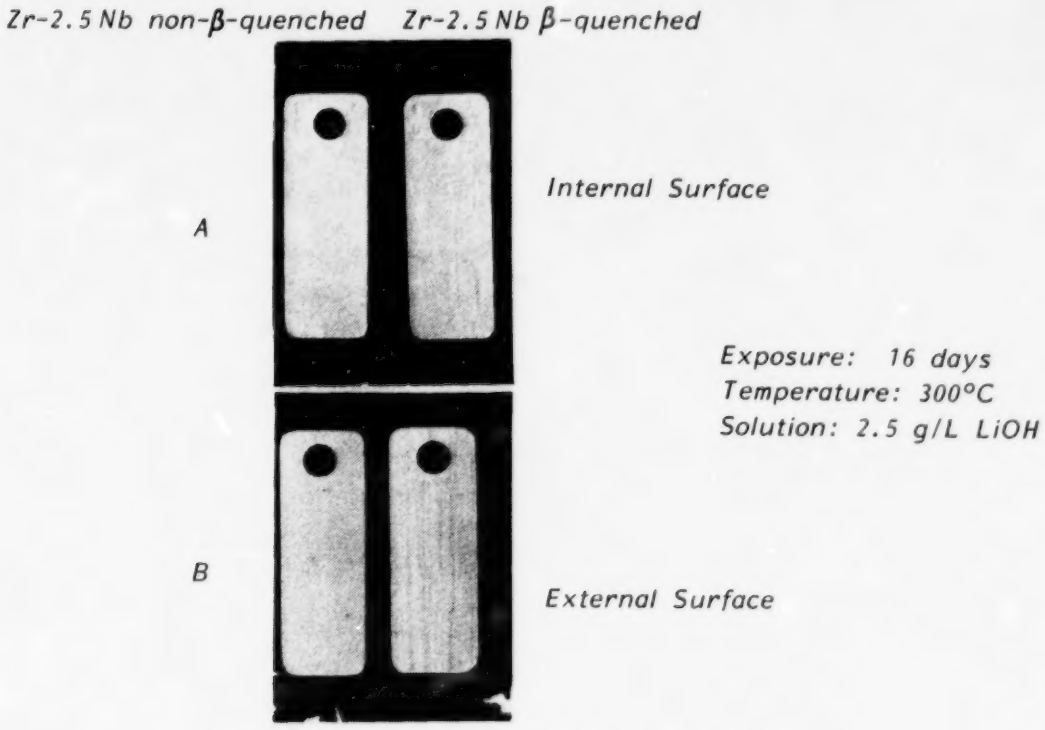

FIGURE 18

TYPICAL SURFACE CONDITION OF P/T CORROSION SAMPLES AFTER CORROSION TEST SHOWING DIFFERENCES BETWEEN INTERNAL AND EXTERNAL SURFACES OF P/Ts

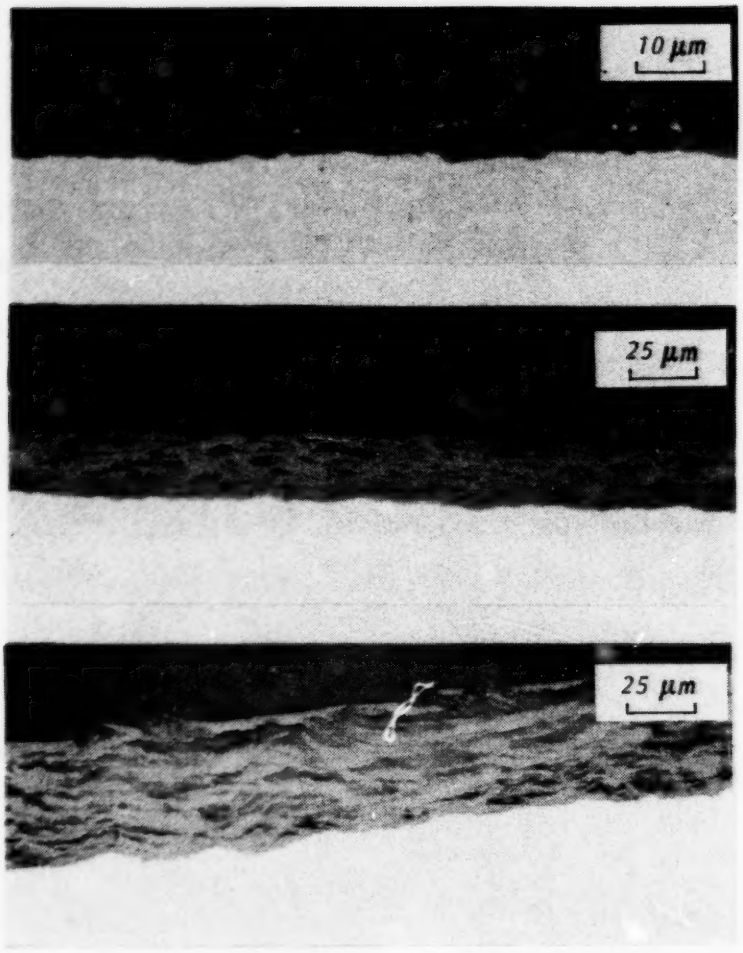

Zr-2.5 Nb
β-quenched

A Exposure: 40 days
Temperature: 340°C
Solution: 0.5 g/L

Zr-2.5 Nb
β-quenched

B Exposure: 11 days
Temperature: 340°C
Solution: 1 g/L

Zr-2.5 Nb
non-β-quenched

C Exposure: 9 days
Temperature: 340°C
Solution: 2.5 g/L

FIGURE 19

TYPICAL CROSS SECTIONS OF OXIDE SCALE ON CORROSION SAMPLES
AFTER EXPOSURE TO DIFFERENT EXPERIMENTAL CONDITIONS

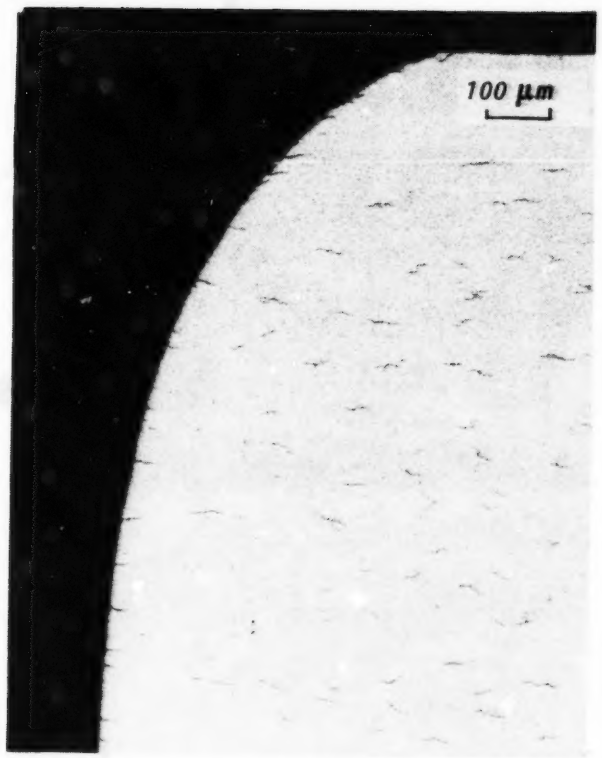

Exposure: 40 days
Temperature: 340°C
Solution: 0.5 g/L

FIGURE 20

TYPICAL CROSS SECTION OF OXIDE SCALE FORMED ON Zr-2.5 Nb β-QUENCHED SHOWING THE SCALE ADHERENCE AT METAL/OXIDE INTERFACE

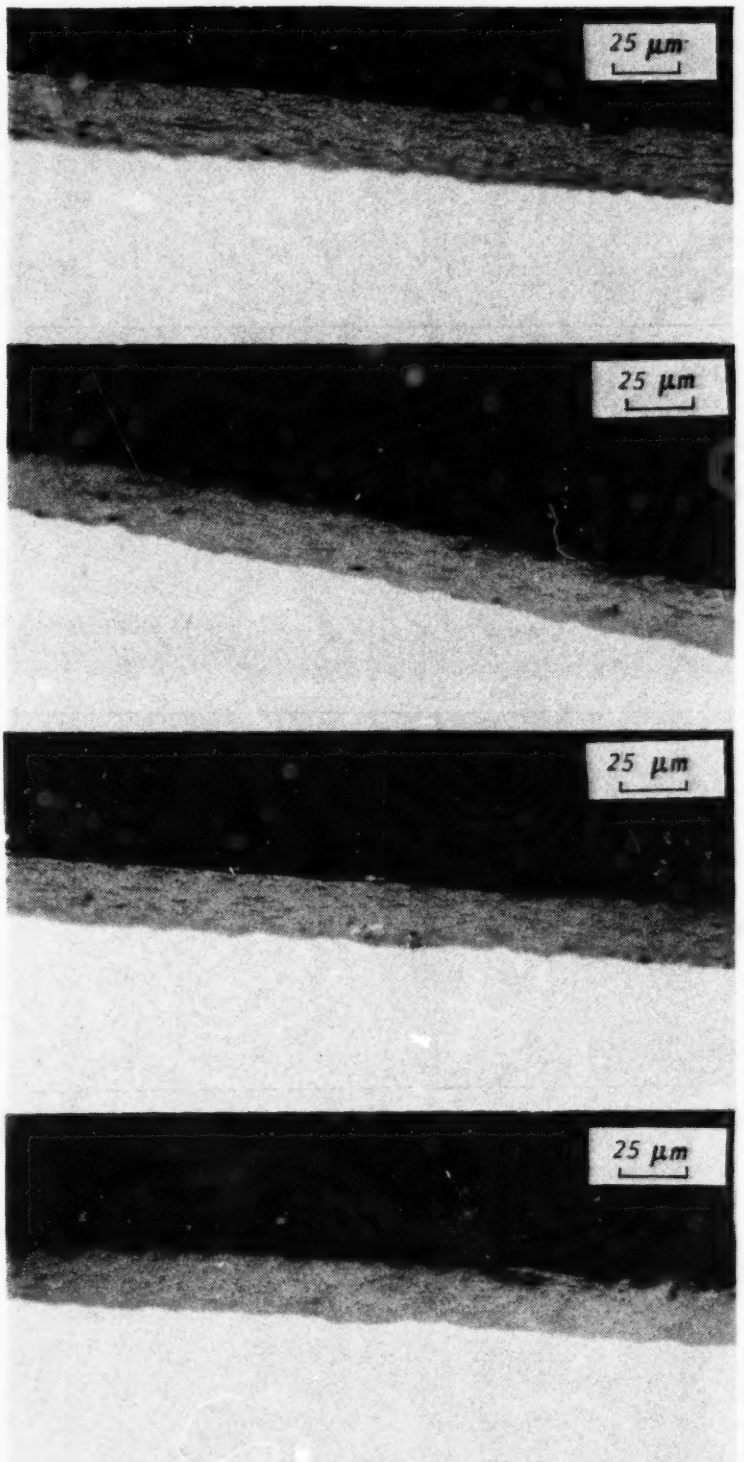

FIGURE 21

TYPICAL CROSS SECTIONS OF OXIDE SCALE FORMED ON CORROSION SAMPLES AFTER 6 DAYS EXPOSURE IN 2.5 g/L LiOH AT 340°C SHOWING EFFECT OF MATERIAL ON SCALE POROSITY AND INTEGRITY

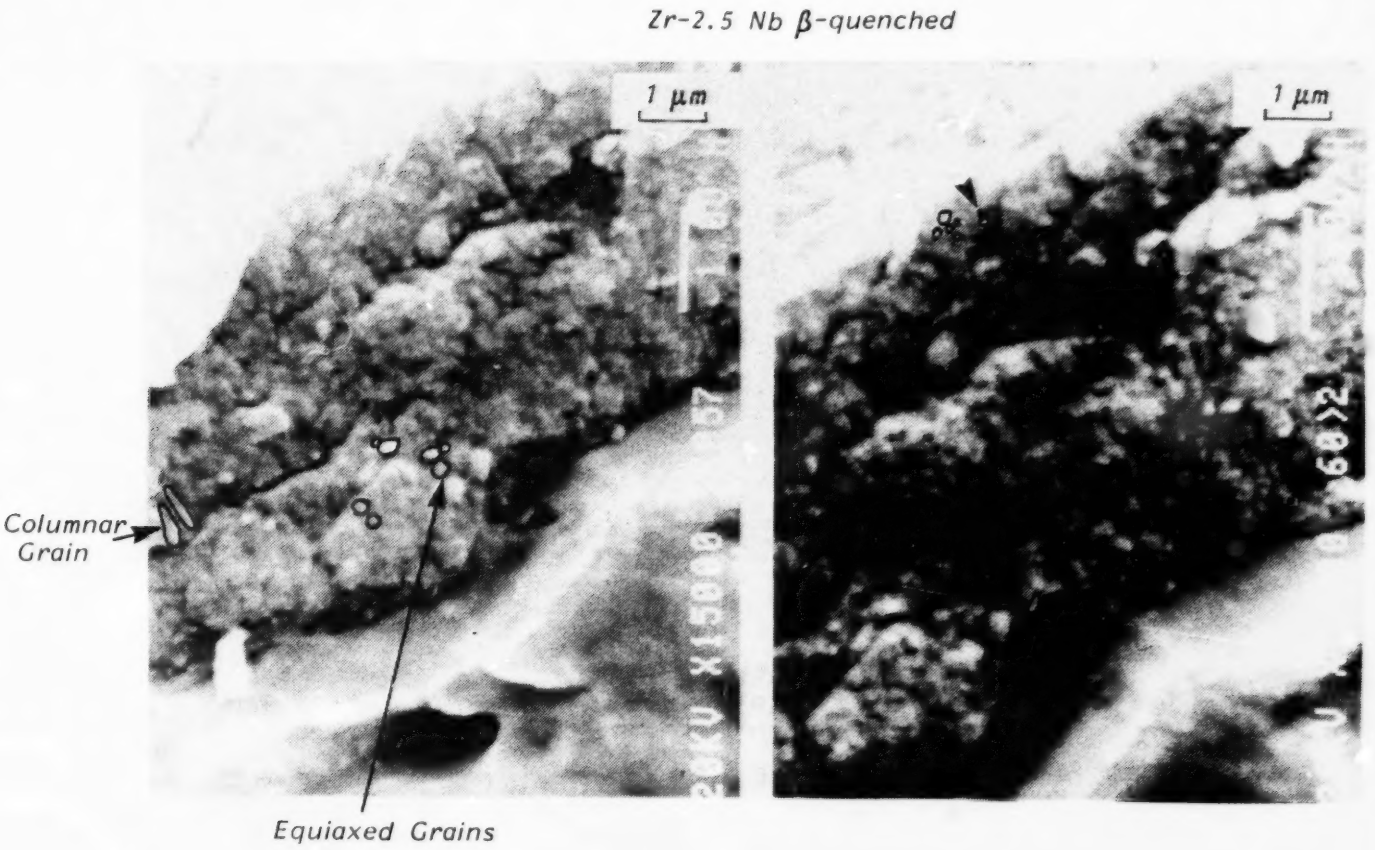

FIGURE 22

SCANNING ELECTRON MICROGRAPHS SHOWING THE FRACTURE SURFACE OF THE CORROSION SCALE AFTER 40 DAY EXPOSURE TEST IN 0.5 g/L LiOH SOLUTION AT 340°C

Zr-2.5 Nb β-quenched

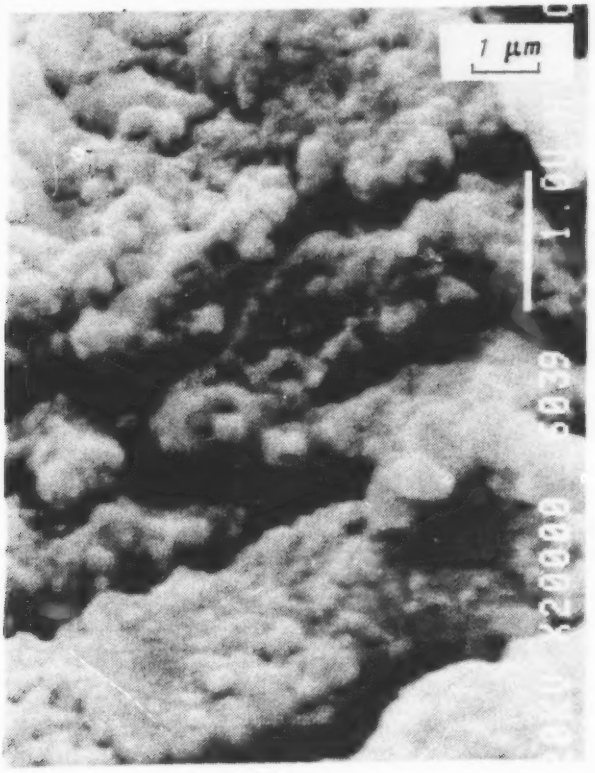

FIGURE 23

SCANNING ELECTRON MICROGRAPH SHOWING THE OUTER PART OF THE FRACTURED CORROSION SCALE AFTER 9 DAY EXPOSURE TEST IN 2.5 g/L LiOH SOLUTION AT 340°C

Zr-2.5 Nb β-quenched

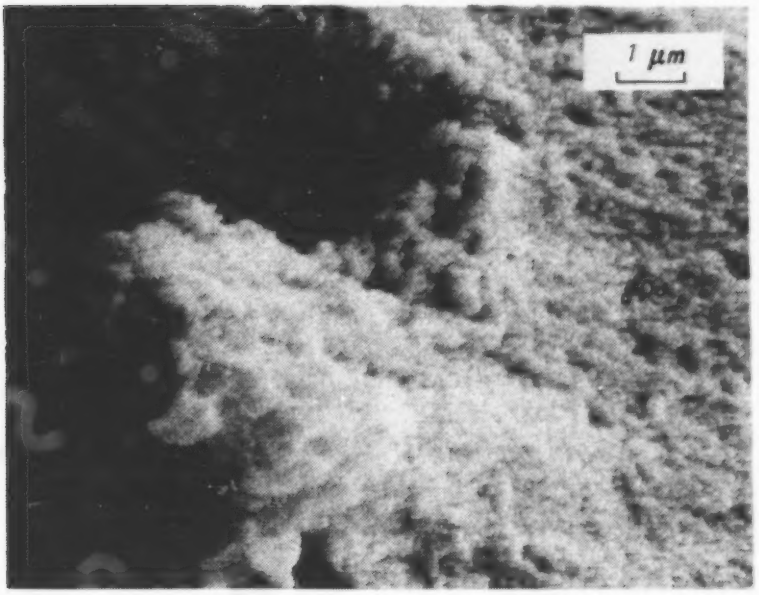

Spherical Grains

FIGURE 24

SCANNING ELECTRON MICROGRAPH SHOWING THE OUTER PART OF THE FRACTURED CORROSION SCALE AFTER 2 DAY EXPOSURE IN 4 g/L LiOH SOLUTION AT 340°C

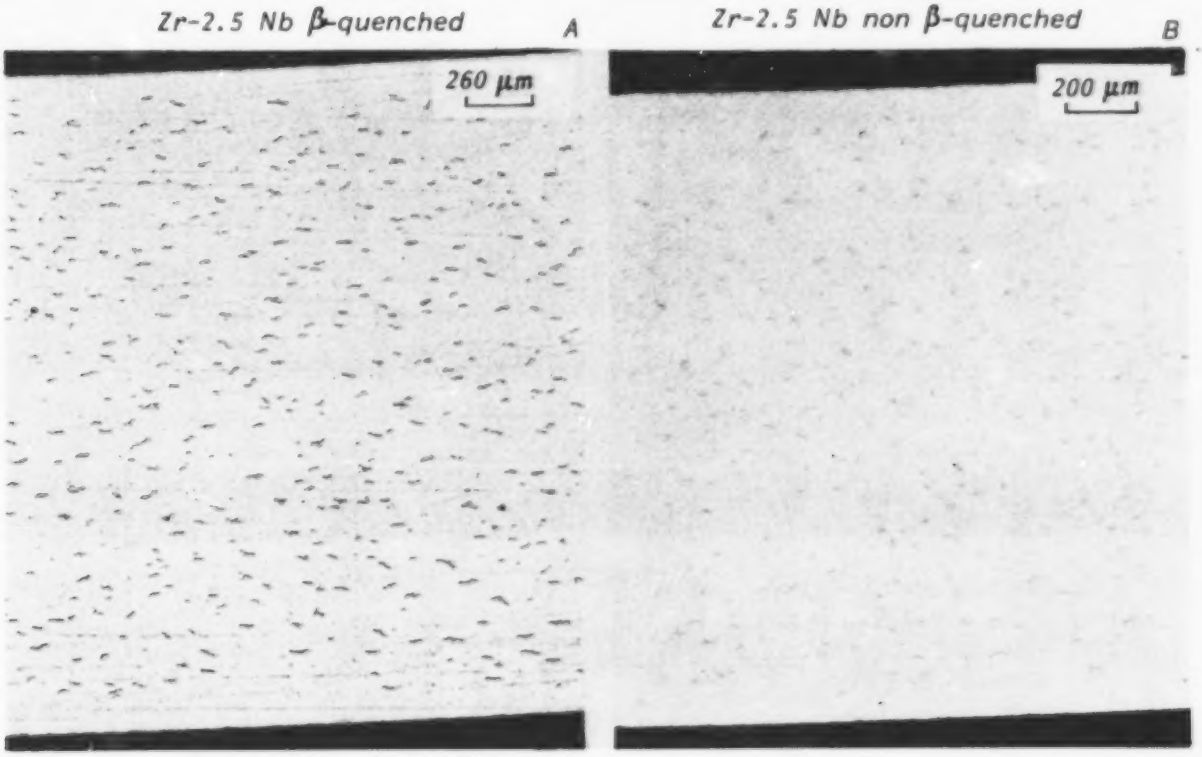

FIGURE 25

HYDRIDE DISTRIBUTION UNDER THE OXIDE SCALE
FORMED ON Zr-2.5 Nb SAMPLES AFTER 40 DAY EXPOSURE
TO 0.5 g/L LiOH SOLUTION AT 340°C

Exposure: 26 days
Temperature: 340°C
Solution: 0.5 g/L

Exposure: 9 days
Temperature: 340°C
Solution: 2.5 g/L

FIGURE 26

TYPICAL CROSS SECTIONS OF THE OXIDE SCALE FORMED ON Zr-2 COUPONS EXPOSED TO LiOH SAMPLES

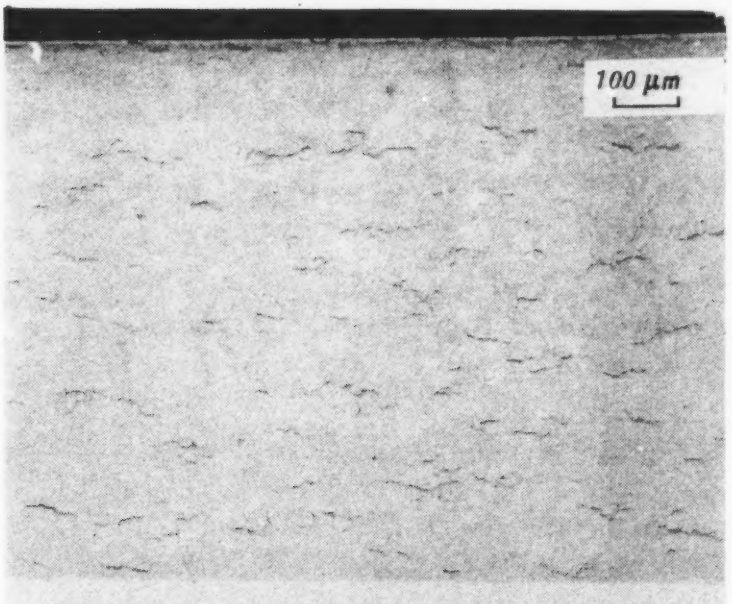

Exposure: 26 days
Temperature: 340°C
Solution: 0.5g/L LiOH

A

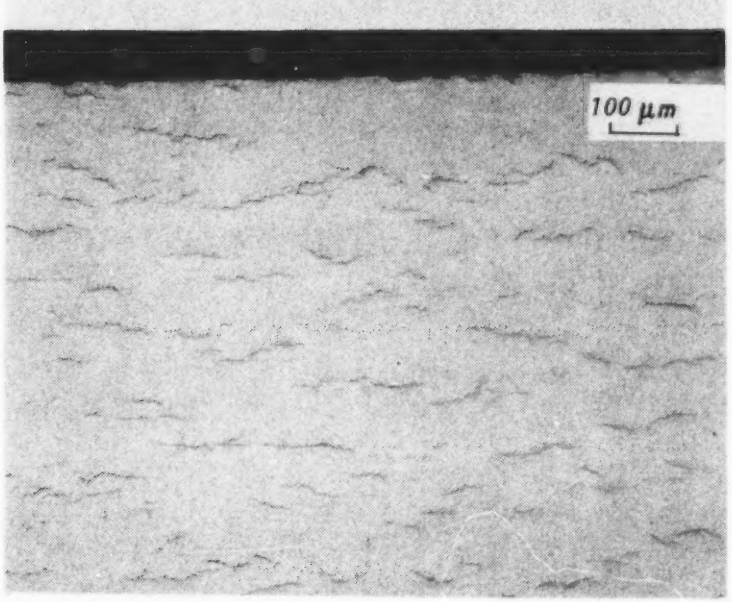

Exposure: 9 days
Temperature: 340°C
Solution: 2.5g/L LiOH

B

FIGURE 27

TYPICAL STRUCTURE OF HYDRIDES UNDER SCALES FORMED ON Zr-2 CORROSION SAMPLES

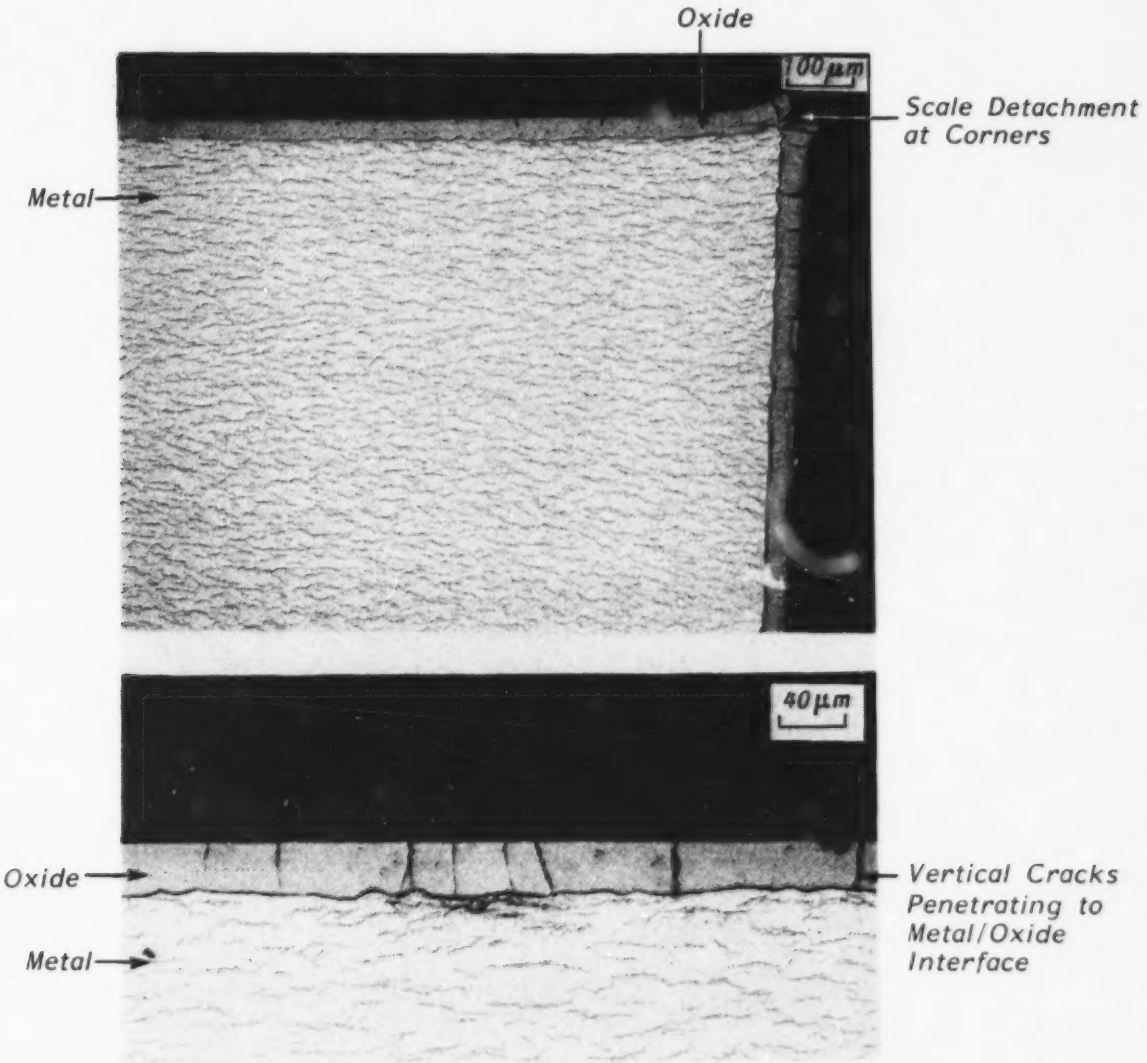

FIGURE 28

TYPICAL CROSS SECTIONS OF Zr-2.5 Nb NON-β-QUENCHED SAMPLE AFTER 32 DAY EXPOSURE IN STEAM AT 490°C, SHOWING OXIDE SCALE MORPHOLOGY AND HYDRIDE STRUCTURE

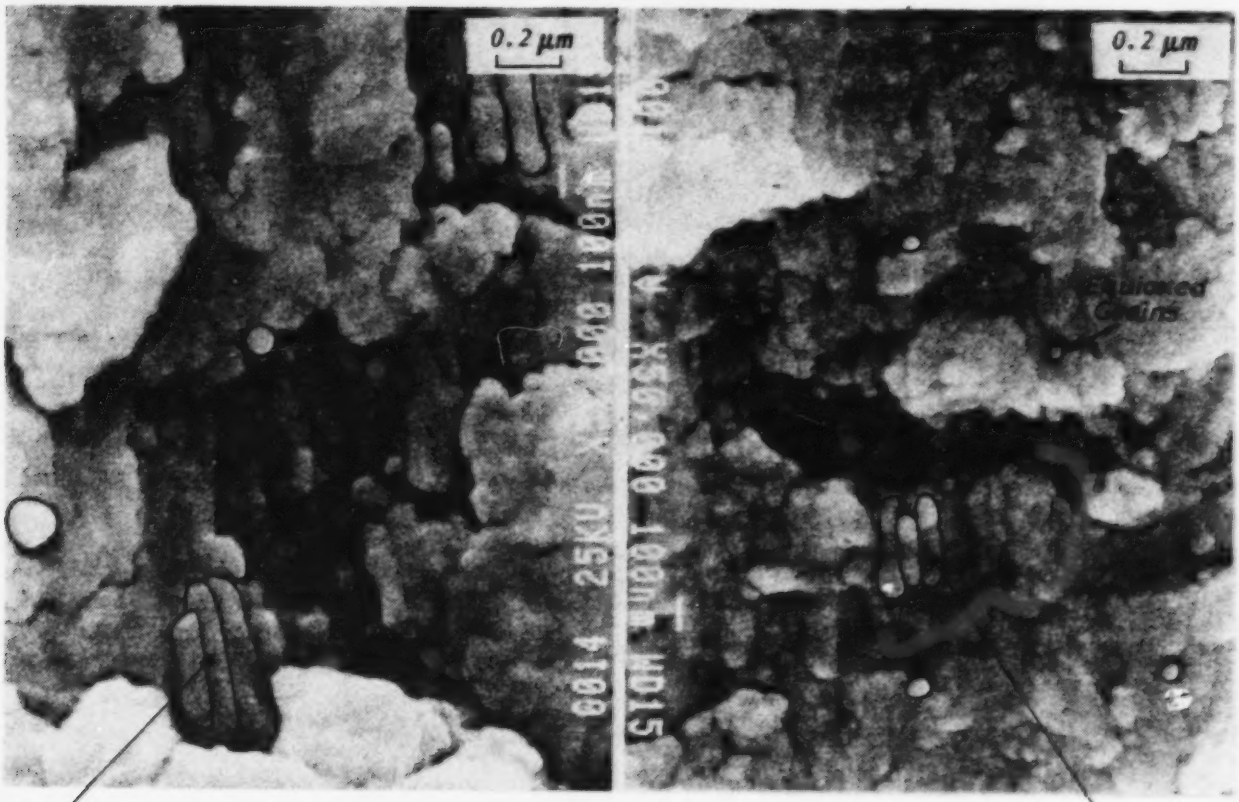

FIGURE 29

TYPICAL SCANNING ELECTRON MICROGRAPHS OF FRACTURE SURFACE OF STEAM-FORMED SCALE

171811 RD

DISTRIBUTION

--Mr. H. Isaac	Design & Devel- Gen, H11G27
--Dr. D. Mills	Director of Research
--Mr. B. Montford	Tech & Trg Ser, A7H9
Mr. M.W. Shanahan	Tech & Trg Ser, A7H8
Mr. R.G. Barton	Tech & Trg Ser, A7G9
Dr. G.J. Field	Design & Devel - Gen, H10A16
Mr. J.S. Li	Design & Devel - Gen, H11E27
Mr. R.E. Heathcock	Design & Devel - Gen, H11G26
Mr. R.Y. Lior	Design & Devel - Gen, H10E16
Mrs. E.G. Csillag	Design & Devel - Gen, H11E25
Mr. M. Hardie	Design & Devel - Gen, H10C16
Dr. B. Cox	AECL - CRNL
Mr. V. Urbanic	AECL - CRNL
Ms. T. Gendron	AECL - CRNL
Mr. A. Shaddick	AECL - CRNL
Mr. E.G. Price	AECL - CO
Mr. V. Murphy	AECL - CO
Dr. C.K. Chow	AECL - WNRE
Mrs. L.G. Woodworth	AECL - WNRE
Mr. F.W. Stanley	AECL - WNRE
Dr. C.J. Simpson	Divisional Projects Dept
Dr. R.J. Fleck	Metallurgical Research
Dr. J.A. Baron	Metallurgical Research
Dr. S. Lawson	Metallurgical Research
Dr. P.C. Lichtenberger	Metallurgical Research
Dr. P. Mayer	Metallurgical Research
Dr. B.D. Warr	Metallurgical Research
Mr. E.M. Rasile	Metallurgical Research
Dr. A.V. Manolescu	Metallurgical Research

Public Reference Centre
Editorial Copy (2)
Office Copies (3)
Extra Copies (3)

--Executive Summary Only

- last page -